ン誘導作用が低いものの，発生したキャビテーション気泡の直径は小さく，細胞傷害性は低いと考えられている．そのため，1–2 MHz の超音波周波数が遺伝子導入に使用されるようになった．しかし，この周波数ではキャビテーション誘導の閾値が高くなるため，強い照射強度（20–100 W/cm²）あるいは長い時間（3–30 分）の照射が必要となり細胞傷害の問題を完全に払拭できるような条件と言い難かった．この問題を解決するために考えられたのが，超音波によるキャビテーションを誘導し易くするためにあらかじめキャビテーション核となる微小気泡を存在させておくことである．すなわち，上述の超音波遺伝子導入において超音波造影剤であるマイクロバブルを添加することで，低い超音波照射強度及び短時間で遺伝子導入可能であることが報告されるようになった．[13] これは，マイクロバブルがキャビテーション核として存在することで，遺伝子導入に必要なキャビテーションを誘導するための超音波照射強度の閾値を下げることができたと考えられた (Fig. 2)．このような背景の下，1990 年代後半からマイクロバブルと超音波の併用による遺伝子導入に関する研究がスタートしている．

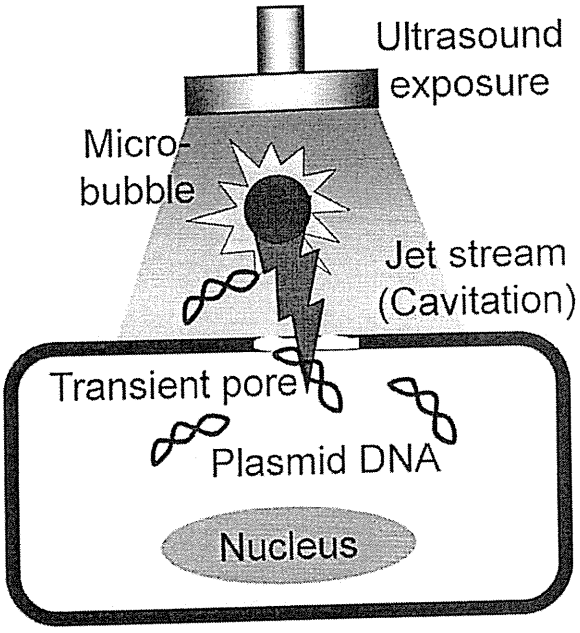

Fig. 2. Mechanism of Gene Delivery into Cell by Microbubble and Ultrasound Exposure

4. 微小気泡と超音波の併用による遺伝子デリバリー

マイクロバブルを用いた遺伝子導入増強に関する報告が進む中，マイクロバブルの種類による導入効率の比較検討も行われた．アルブミン外殻中に空気を封入した Albunex，アルブミン外殻中にパーフルオロプロパンを封入した Optison，アルブミン外殻中に空気とパーフルオロプロパンを封入した PESDA，パルミチン酸を含むガラクトース結晶複合体からなる Levovist，脂質膜中にパーフルオロプロパンを封入した Definity など多くの超音波造影剤が開発されており，各々のマイクロバブルと超音波の併用による遺伝子導入の増強効果が認められている．[14] このようなキャビテーションを利用したデリバリーシステムは，体外からの超音波照射により目的組織にのみ低侵襲的な遺伝子デリバリーを可能とする新たな遺伝子デリバリーシステムとして期待されている．そこで，このキャビテーションを利用した遺伝子導入がバブルリポソームでも可能であることを評価するため，バブルリポソームと超音波照射の併用による遺伝子導入について検討した．様々な種類の細胞にルシフェラーゼ発現プラスミド DNA を超音波単独又はバブルリポソームと超音波照射の併用により遺伝子導入したところ，いずれの細胞種においてもバブルリポソームと超音波照射の併用により高いルシフェラーゼ発現が認められた（Fig. 3)．[11] このようにバブルリポソームと超音波の併用が細胞種を問わず遺伝子導入可能であったのは，キャビテーションによる物理的エネルギーを利用して細胞質内に遺伝子を直接導入できるためであると考えられた．

本方法は超音波を照射したときのみ遺伝子導入が誘導されるため，超音波照射部位をコントロールすることで超音波照射部位特異的な遺伝子導入が可能になると考えられる．そこで，バブルリポソームと超音波の併用による低侵襲的かつ組織特異的な *in vivo* 遺伝子導入システムの確立を試みた．バブルリポソームとルシフェラーゼ発現プラスミド DNA をマウスの尾静脈から全身投与後，直ちに肝臓に向けて体外から経皮的に超音波照射した．その 2 日後にマウスから各臓器を回収し，ルシフェラーゼ活性を測定した（Fig. 4)．その結果，超音波照射部位である肝臓において高いルシフェラーゼ発現が認め

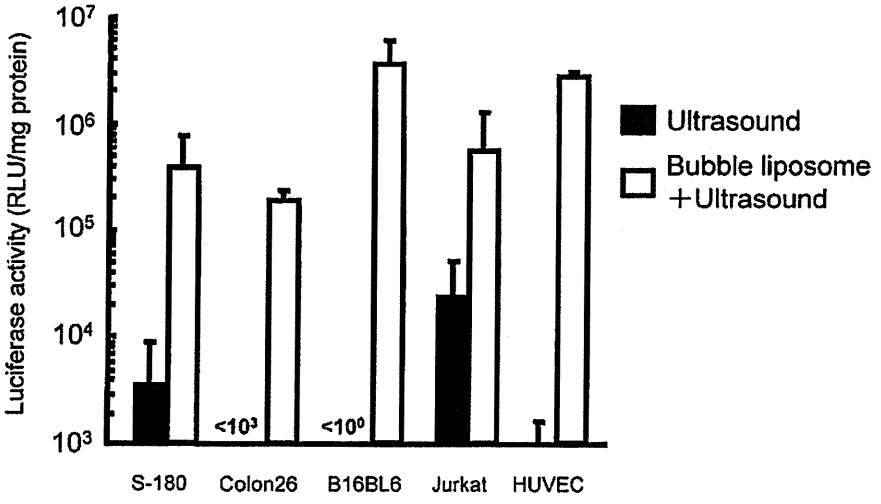

Fig. 3. Gene Delivery by Bubble Liposome and Ultrasound Exposure *in vitro*

Cells (1×10^5 cells/500 μl) mixed with pCMV-Luc (5 μg) and Bubble liposomes (60 μg) were exposed or not to ultrasound (frequency, 2 MHz; duty, 50%; burst rate, 2 Hz; intensity, 2.5 W/cm^2; time, 10 s). The cells were washed and cultured for 2 days. Thereafter, luciferase activity was determined. Data are shown as means±S.D. (n=3). S-180, mouse sarcoma; Colon26, mouse colon adenocarcinoma; B16BL6, mouse melanoma; Jurkat, human T cell line; HUVEC, human umbilical vein endothelial cell.

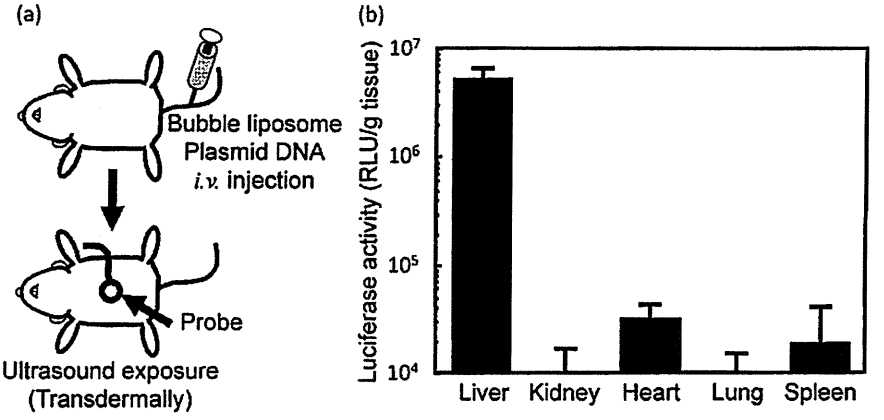

Fig. 4. Liver Specific Gene Delivery by Bubble Liposomes and Ultrasound Exposure

(a) Gene delivery method: Luciferase corded plasmid DNA (100 μg) and Bubble liposomes (500 μg) were intravenously injected and ultrasound (1 MHz, 1 W/cm^2, 1 min) was transdermally exposed toward liver. After 1 day of ultrasound exposure, luciferase expression in each tissue was measured. (b) Luciferase expression in each tissue.

られた．このようにバブルリポソームとプラスミドDNAが血流を介して流れていたにもかかわらず肝臓に遺伝子導入できたのは，超音波照射部位である肝臓でバブルリポソームがキャビテーションを誘導し，そのときに遺伝子を肝臓に導入したためであると考えられた．今回は示していないが，筆者らは同様の方法を用い超音波照射部位を変更することで脾臓や脳へも遺伝子導入できることを確認している．このように今回示した方法は，超音波照射部位を変更するだけで様々な組織や部位に低侵襲的かつ特異的に遺伝子導入できる可能性を有しており，他の遺伝子導入ベクターにはない非常に簡便でユニークな特性を持つ方法であると言える．

5. バブルリポソームと超音波照射を利用したがん遺伝子療法

近年，抗腫瘍免疫の活性化を目的とした新しいがん治療法としてサイトカイン療法が注目されている．その中でもIL-12は，NK細胞や細胞傷害性T細胞などを活性化することで強力な抗腫瘍効果を誘導するサイトカインとして，臨床の場においても期

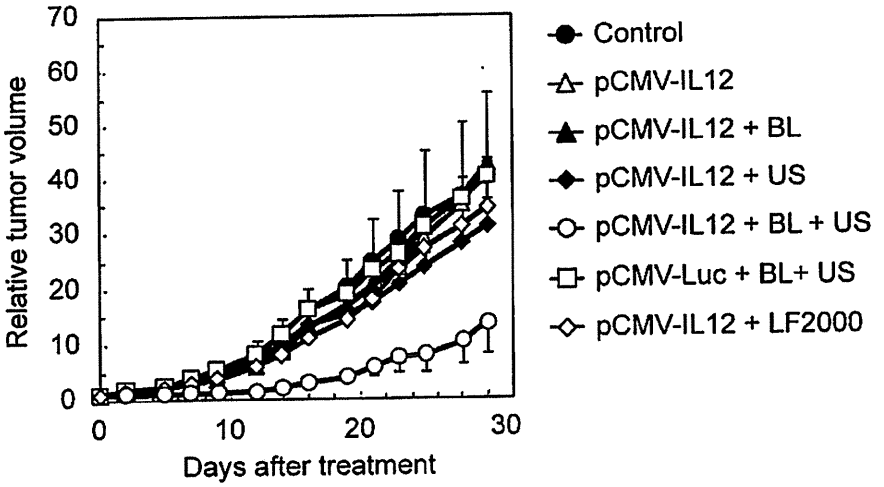

Fig. 5. Cancer Gene Therapy in Gene Delivery by Bubble Liposomes and Ultrasound Exposure

B6C3F1 mice were intradermally inoculated with 1×10^6 OV-HM cells into the flank. After 7 days of tumor inoculation, the tumors were injected with pCMV-IL12 (10 μg) using Bubble liposomes (2.5 μg) and/or ultrasound (1 MHz, 0.7 W/cm^2, 1 min), or Lipofectamine 2000 as a conventional lipofection method. The volume of the growing tumors was calculated by: (tumor volume; mm^3) = (major axis; mm) $\times$ (minor axis; mm)$^2\times0.5$. The data are represented as tumor volume relative to the tumor volume on the first day of treatment (day 7 after tumor inoculation). Each point represents the mean$\pm$S.D. (n=5). BL, Bubble liposomes; US, Ultrasound; LF2000, Lipofectamine 2000.

待されている．しかし，IL-12 の全身投与は，全身作用による副作用のリスクが懸念されており，副作用の影響なく治療効果を得るためには，がん組織特異的に IL-12 を作用させる必要がある．前項で示したように，バブルリポソームと超音波照射の併用は，がん細胞に効率よく遺伝子導入できることが明らかとなっている．そこで筆者らは，バブルリポソームと超音波の併用による IL-12 発現プラスミド DNA（pCMV-IL12）の遺伝子導入によるがん遺伝子治療を試みた（Fig. 5）．その結果，バブルリポソームと超音波の併用により pCMV-IL12 を導入した群で顕著な腫瘍増殖抑制効果が認められた．[7] 一方，Lipofectamine™ 2000 による遺伝子導入では，ほとんど腫瘍増殖抑制効果は認められなかった．このような結果が得られたのは，バブルリポソームと超音波の併用により効率よく IL-12 遺伝子が発現し，強力な抗腫瘍免疫が誘導されたためであると考えられた．このことから，バブルリポソームと超音波照射の併用法は IL-12 がん遺伝子治療において有用な非ウイルスベクターになることが示唆された．

6. おわりに

本稿では，バブルリポソームと超音波を利用した遺伝子導入について紹介した．バブルリポソームと超音波の併用による遺伝子導入は，短時間の超音波照射で細胞内に遺伝子導入可能である上，体外からの超音波照射により超音波照射部位のみに遺伝子を送達可能であった．本方法は既存の非ウイルスベクターシステムとは異なり，低侵襲的かつ部位特異的遺伝子導入を可能とする有望な遺伝子導入法として期待される．それゆえ，本稿で紹介した方法は，遺伝子治療分野で課題となっている部位特異的な遺伝子発現用ベクター開発において有望な技術ではないかと考えられる．

冒頭でも述べたようにバブルリポソームはリポソーム技術を基盤としたバブル製剤であり，リポソーム表面に容易に標的指向性分子を修飾することができる．今回紹介しなかったが，これまでに筆者らの共同研究者はバブルリポソーム表面に血栓を認識するペプチドを修飾し，血栓モデル動物に静脈内投与することで，バブルリポソームの血栓部位への集積を超音波造影により確認している．[4] さらに，この集積したバブルリポソームにキャビテーションを誘導するような周波数・強度の超音波を体外から照射することで血栓を破壊し血流を再開することが可能であることも確認している．このように，バブルリポソームと超音波の併用は，単に細胞に遺伝子を導入するだけでなく，これまで超音波造影では診断できなかった血栓の診断を可能にし，さらに治療用超音波照射により血栓治療も行えるような次世代型医療システムの構築を予感させる．

今後，バブルリポソームへのパッシブターゲティングやアクティブターゲティング能の付与による体内動態制御及び集束超音波による超音波照射部位の空間的制御の両者を組み合わせたダブルターゲティングを利用することで，厳密な空間的・時間的制御を可能とする理想的な超音波がん治療システムが構築可能になるものと期待される．

謝辞　本稿で紹介したバブルリポソームに関する研究は，帝京大学薬学部生物薬剤学教室で行われた研究であり，研究遂行にご協力頂いた学生諸子に深謝する．また，本研究遂行においてご協力頂いた東京薬科大学薬学部・根岸洋一先生，国立がんセンター東病院・松村保広先生，陸上自衛隊研究本部・萩沢康介博士，福岡大学医学部・立花克郎先生，北海道大学大学院情報科学研究科・工藤信樹先生に深謝する．さらに，本研究の一部は厚労省科研費：第3次対がん総合戦略研究事業，文科省科研費：基盤研究（A），若手研究（B），医薬基盤研究所：保健医療分野における基礎研究推進事業の研究助成により遂行された研究である．

REFERENCES

1) Harata M., Soda Y., Tani K., Ooi J., Takizawa T., Chen M., Bai Y., Izawa K., Kobayashi S., Tomonari A., Nagamura F., Takahashi S., Uchimaru K., Iseki T., Tsuji T., Takahashi T. A., Sugita K., Nakazawa S., Tojo A., Maruyama K., Asano S., *Blood*, **104**, 1442–1449 (2004).
2) Suzuki R., Takizawa T., Kuwata Y., Mutoh M., Ishiguro N., Utoguchi N., Shinohara A., Eriguchi M., Yanagie H., Maruyama K., *Int. J. Pharm.*, **346**, 143–150 (2008).
3) Yanagie H., Maruyama K., Takizawa T., Ishida O., Ogura K., Matsumoto T., Sakurai Y., Kobayashi T., Shinohara A., Rant J., Skvarc J., Ilic R., Kuhne G., Chiba M., Furuya Y., Sugiyama H., Hisa T., Ono K., Kobayashi H., Eriguchi M., *Biomed. Pharmacother.*, **60**, 43–50 (2006).
4) Hagisawa K., Nishioka T., Suzuki R., Takizawa T., Maruyama K., Takase B., Ishihara M., Kurita A., Yoshimoto N., Ohsuzu F., Kikuchi M., *Int. J. Cardiol.* (in press)
5) Un K., Kawakami S., Suzuki R., Maruyama K., Yamashita F., Hashida M., *Hum. Gene Ther.*, **21**, 65–74 (2010).
6) Negishi Y., Omata D., Iijima H., Takabayashi Y., Suzuki K., Endo Y., Suzuki R., Maruyama K., Nomizu M., Aramaki Y., *Mol. Pharm.*, **7**, 217–226 (2010).
7) Suzuki R., Namai E., Oda Y., Nishiie N., Otake S., Koshima R., Hirata K., Taira Y., Utoguchi N., Negishi Y., Nakagawa S., Maruyama K., *J. Control. Release*, **142**, 245–250 (2010).
8) Suzuki R., Oda Y., Utoguchi N., Namai E., Taira Y., Okada N., Kadowaki N., Kodama T., Tachibana K., Maruyama K., *J. Control. Release*, **133**, 198–205 (2009).
9) Suzuki R., Takizawa T., Negishi Y., Utoguchi N., Sawamura K., Tanaka K., Namai E., Oda Y., Matsumura Y., Maruyama K., *J. Control. Release*, **125**, 137–144 (2008).
10) Negishi Y., Endo Y., Fukuyama T., Suzuki R., Takizawa T., Omata D., Maruyama K., Aramaki Y., *J. Control. Release*, **132**, 124–130 (2008).
11) Suzuki R., Takizawa T., Negishi Y., Utoguchi N., Maruyama K., *J. Drug. Target.*, **15**, 531–537 (2007).
12) Fechheimer M., Boylan J. F., Parker S., Sisken J. E., Patel G. L., Zimmer S. G., *Proc. Natl. Acad. Sci. USA*, **84**, 8463–8467 (1987).
13) Suzuki R., Oda Y., Utoguchi N., Maruyama K., *J. Control. Release.* (in press)
14) Li T., Tachibana K., Kuroki M., *Radiology*, **229**, 423–428 (2003).

YAKUGAKU ZASSHI 130(11) 1489—1496 (2010) © 2010 The Pharmaceutical Society of Japan

—Review—

バブルリポソームと超音波技術を融合した骨格筋への遺伝子デリバリーシステムの開発

根岸洋一,*,[a] 高橋(遠藤)葉子,[a] 鈴木　亮,[b] 丸山一雄,[b] 新槇幸彦[a]

Development of Gene Delivery System into Skeletal Muscles by Bubble Liposomes and Ultrasound

Yoichi NEGISHI,*,[a] Yoko ENDO-TAKAHASHI,[a] Ryo SUZUKI,[b] Kazuo MARUYAMA,[b] and Yukihiko ARAMAKI[a]

[a]*Department of Drug and Gene Delivery Systems, School of Pharmacy, Tokyo University of Pharmacy and Life Sciences, 1432-1 Horinouchi, Hachioji, Tokyo 192-0392, Japan, and* [b]*Department of Biopharmaceutics, School of Pharmaceutical Sciences, Teikyo University, 1091-1 Suwarashi, Midori-ku, Sagamihara 252-5195, Japan*

(Received July 20, 2010)

Skeletal muscle is a promising target tissue for the gene therapy of both muscle and non-muscle disorders. Gene transfer into muscle tissue can produce a variety of physiologically active proteins and may ultimately be applied to treatment of many diseases. A variety of methods have been studied to transfer genes into skeletal muscle, including viral and non-viral vectors. Recently, we have developed the polyethyleneglycol (PEG)-modified liposomes entrapping echo-contrast gas known as ultrasound (US) imaging gas. We have called the liposomes "Bubble liposomes" (BLs). We have further demonstrated that US-mediated eruption of BLs loaded with naked plasmid-DNA is a feasible and efficient technique for gene delivery. In this study, to assess the feasibility and the effectiveness of BLs for the gene therapy of disorders, we tried to deliver therapeutic genes (anti-inflammatory cytokine; IL-10 or anti-angiogenic factor; hK1-5) into skeletal muscles of arthritis or tumor model mice by the gene delivery system with BLs and US exposure. As a result, their disease symptom was efficiently improved by the systemic secretion of therapeutic proteins. Thus, this US-mediated BLs technique for muscle gene transfer may provide an effective noninvasive method for arthritis or cancer gene therapy in clinical use. In addition, it may be applicable for the gene therapy of other non-muscle and muscle disorders.

Key words——ultrasound; Bubble liposome; gene delivery system; gene therapy

1. はじめに

遺伝子治療は，候補となる治療用遺伝子を体内の標的組織へ，効率的に安全に導入する手法を用いて，遺伝病，がん，感染症などの疾患へ適用する治療法で臨床応用が期待されている．標的組織への遺伝子導入を担うベクターの開発は，遺伝子治療の技術開発の中でも重要であると考えられているが，毒性，抗原性などの臨床上の安全性に問題がなく，しかも遺伝子発現効率の高い非ウイルスベクター及びドラッグデリバリーシステム（DDS）技術・方法論の研究開発が切望されている．[1,2]

そのような背景から，これまでにわれわれは，非ウイルスベクターの新規の遺伝子デリバリーツールとしての超音波造影ガス封入リポソーム（バブルリポソーム）[3-7]と超音波照射を利用した遺伝子デリバリーシステムの開発を進めてきた．

本稿では，バブルリポソームを利用した骨格筋への超音波遺伝子デリバリー技術を紹介し，遺伝子治療に向けた応用展開について概説する．

2. 超音波造影ガス封入リポソーム（バブルリポソーム）

超音波は，組織ダメージが極めて低く安全性が高いことから，既に医療分野で非侵襲的な超音波診断・治療などに利用されている．近年では，超音波エネルギーのDDSへの応用が考案され，実際に超音波造影剤であるマイクロバブルと導入遺伝子の共

[a]東京薬科大学薬学部薬物送達学教室（〒192-0392 東京都八王子市堀之内1432-1），[b]帝京大学薬学部生物薬剤学教室（〒252-5195 神奈川県相模原市緑区寸沢嵐1091-1）
*e-mail: negishi@toyaku.ac.jp
本総説は，日本薬学会第130年会シンポジウムS19で発表したものを中心に記述したものである．

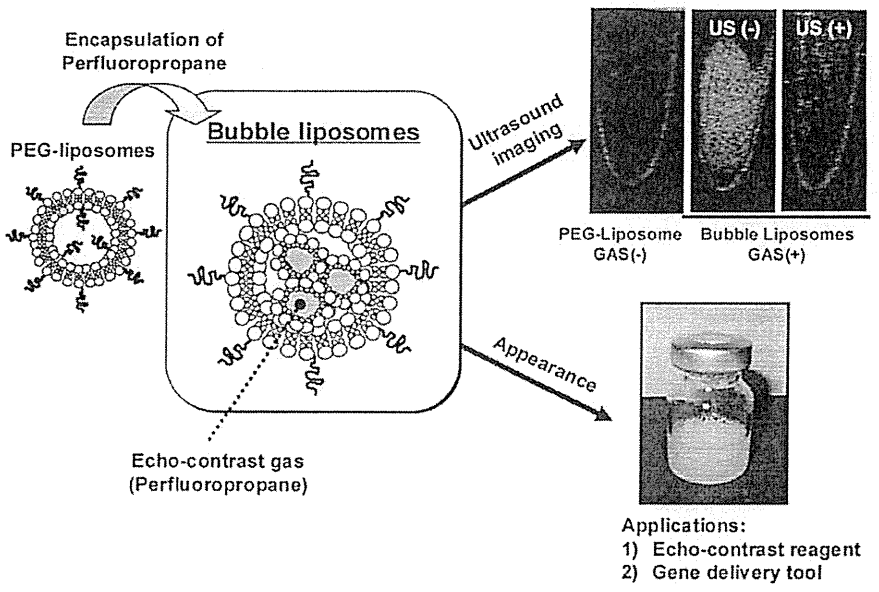

Fig. 1. Bubble Liposomes

存下に治療用超音波を照射することでバブルが崩壊し，同時にキャビテーション（衝撃波）が生じ，その駆動力を利用して薬物や遺伝子を細胞内へと導入する試みが，基礎研究で成功を収めている.[8,9] この方法は，超音波照射した部位にのみ効率よく導入可能であり，臓器・組織特異的に遺伝子導入する方法として期待されている.[10,11] しかし，これまで報告されているマイクロバブルは直径 4–6 μm と粒子サイズが大きいため，組織深部への移行性が悪く，血管内投与に最適なサイズとは言えない．また，表面修飾ができないため，標的指向性が得られないなどの改善すべき課題が残されている.

そのような背景から，これまでに生体適合性・血中安定性・滞留性に優れ，深部組織にまで十分到達できることが報告されている粒子サイズ約 100–200 nm のポリエチレングリコール修飾リポソーム（PEG-リポソーム）[12]に注目し，PEG-リポソームに超音波造影ガスであるパーフルオロプロパンを封入したバブルリポソームを調製した（Fig. 1）．これは，超音波造影剤として機能するのみならず，治療用超音波（1–3 MHz）を併用する低侵襲的な薬物・遺伝子デリバリーツールとして期待される（Fig. 2）.[3,4] さらにリポソームは，様々な修飾をすることで標的指向性を付与できることが知られている．以上より，バブルリポソームはマイクロバブルの問題を解決し得る新規の遺伝子デリバリーツールとなると考えられる.

3. バブルリポソームを利用した超音波遺伝子デリバリーシステム

既存のマイクロバブルに超音波照射を行うとバブル崩壊に伴うキャビテーション誘導が生じ，それを駆動力とする薬物や遺伝子の細胞内導入法が報告されている．そこで，まず，バブルリポソームのキャビテーション誘導について検討した．試験管内で調製されたバブルリポソームに超音波照射（1–3 MHz）を行うと超音波造影シグナルの減弱が観察された．このことは，バブルリポソームの崩壊に伴うキャビテーション誘導が生じた可能性を示唆している（Fig. 1）．次にバブルリポソームと超音波照射の併用によるキャビテーションを利用した遺伝子導入が可能か否かを COS7 細胞に対して行った．方法としては，バブルリポソームとルシフェラーゼ発現プラスミド DNA（pDNA）を培地中に添加し，直ちに超音波照射（2 MHz, 2.5 W/cm^2, 10 s）を行った.

根岸洋一

東京薬科大学薬学部薬物送達学教室准教授．博士（薬学）．1965 年東京生まれ．東京薬科大学卒業，北海道大学薬学研究科博士課程修了．㈱SRL 遺伝子解析研究センター勤務，1996 年帝京大学薬学部助手，2004 年東京薬科大学薬学部講師，2007 年より現職．2001 年米国ピッツバーグ大学に留学（Leaf Huang 教授）．超音波技術を融合した DDS・GDS の研究開発に従事.

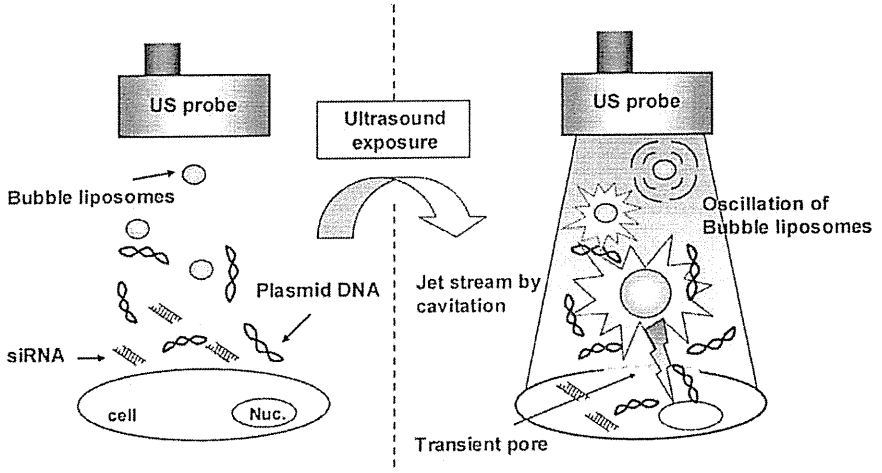

Fig. 2. Mechanism of Gene Delivery System by Bubble Liposomes and Ultrasound

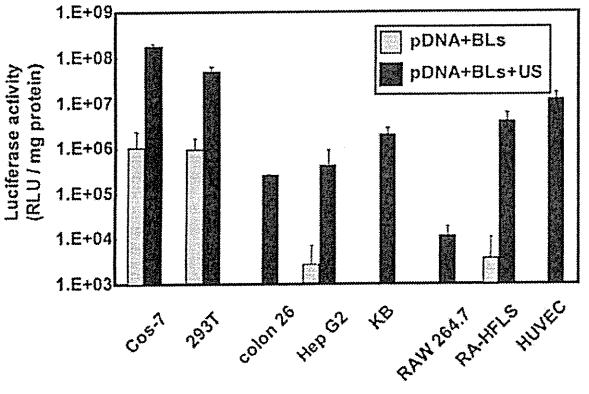

Fig. 3. Transfection with Bubble Liposomes and Ultrasound on Various Cell Lines

Solution of pDNA (pCMV-Luciferase) and Bubble liposomes were added into cells. Immediately, ultrasound (Frequency: 1 MHz, Duty: 50%, Intensity: 2.5 W/cm², Time: 10 s) was exposed. Two days after transfection, luciferase expression was determined.

その結果，ルシフェラーゼ活性の上昇が認められ，細胞内への遺伝子導入は，わずか 10 秒という超音波照射時間で効率よく達成できることが判明した.[3] この効果は pDNA とバブルリポソームの混合液に超音波照射した場合に初めて高い遺伝子発現が認められた．ガス未封入リポソームと超音波照射を併用した場合では，十分な導入効果は得られなかった．COS7 細胞以外のがん細胞（HepG2, Colon26, KB など），関節滑膜細胞，マクロファージ様細胞においても導入効果が示され，バブルリポソームと超音波照射を併用することで種々の培養細胞株に対して遺伝子導入が可能であることが明らかとなった（Fig. 3）．また，本導入システムによって，pDNA のみならず，低分子核酸である siRNA も効率よく細胞内導入できることも明らかとしている.[4]

4. 遺伝子治療における骨格筋への遺伝子デリバリーの有用性

遺伝子治療を成功させるには，生体に対して安全な方法で遺伝子を標的細胞に効率よく導入し，発現させることが重要である.[1,2]

体内の様々な細胞や組織が標的となり得るが，その中でも骨格筋は遺伝子治療の有望な標的組織と考えられている．なぜなら，骨格筋自身が遺伝性疾患（例：筋ジストロフィー）の発症部位で遺伝子治療の標的部位であり，その治療のために有用なタンパク質が骨格筋で発現可能であることが既に示されているからである．さらに，骨格筋には大量の血管が存在するため，局所で発現した生理活性タンパク質を全身へ送り出すことで他の全身性疾患（例：転移性がん，慢性関節リウマチ）の治療が可能となることも理由の 1 つである．また，筋細胞は非分裂細胞なので，細胞分裂に伴う導入遺伝子の消失が回避でき，持続的発現が期待できるという利点もある．これらの特長を生かし，治療効果を最大とするには，治療が必要な部位の筋組織全体若しくは充分な発現量や発現エリアを確保できる範囲に遺伝子導入することが必要である．Figure 4 に示すように治療用遺伝子をバブルリポソームともに筋組織内へと投与した後に，超音波照射することで，バブルリポソームが崩壊し，キャビテーション誘導に伴うマイクロジ

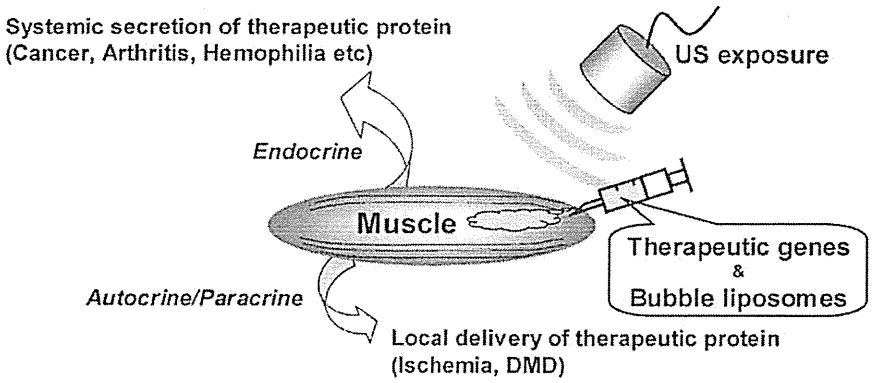

Fig. 4. Gene Delivery System into Muscle by Bubble Liposomes and Ultrasound

エット流を発生させることが可能と考えられる．これを駆動力とすることで，効率のよい筋細胞内への遺伝子デリバリーが可能となり，遺伝子治療に有用かつ安全性の高い遺伝子デリバリーシステムが構築できると考えられる．

5. バブルリポソームを利用した骨格筋への超音波遺伝子デリバリーシステム

超音波照射を併用したバブルリポソームの *in vivo* での機能評価をするために，骨格筋を標的にし，超音波遺伝子導入効率について検討した．方法としてマウスの脛部筋組織にバブルリポソームとルシフェラーゼ遺伝子をコードしたpDNAの混合溶液を局所筋肉内投与し，直ちに，体外から超音波照射（1 MHz, 50% duty, 2 W/cm², 60 s）し，5日後の摘出組織をホモジネートしてルシフェラーゼ活性測定を行った．なお超音波照射装置は，NEPA GENE社製のSONOPORE 3000，又は，Sonitron 2000を使用した．その結果，pDNA単独，pDNAとバブルリポソーム混合液を添加した群，pDNAに超音波照射した群では，ほとんど遺伝子発現に顕著な差が認められなかったのに対し，pDNAとバブルリポソームを混合し，さらに超音波照射した群では，pDNAなどの上述の群に比べ両組織ともに10倍以上の高い遺伝子発現が認められた（Fig. 5）．さらに遺伝子導入後のpDNAの体内動態並びに発現分布を解析するために，*in vivo* ルシフェラーゼイメージングシステム（IVIS社）を用いた全身での発現分布を解析した．その結果，pDNAのみを導入した場合に比べ，pDNAとバブルリポソーム混合液を局所投与したマウス頚部筋組織において局在化したルシフェラーゼの遺伝子発現の増強が観察

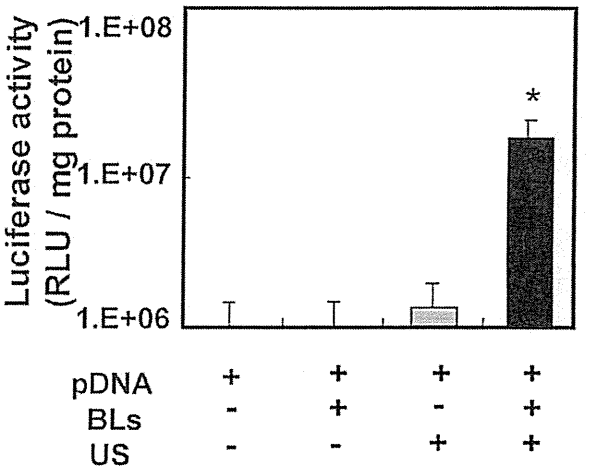

Fig. 5. Luciferase Expression in Muscle Transfected with Bubble Liposomes and Ultrasound

Mice were injected into tibialis muscle with pDNA (pCMV-Luciferase) 10 μg and Bubble liposomes 30 μg. Immediately, ultrasound (Frequency: 1 MHz, Duty: 50%, Intensity: 2 W/cm², Time: 60 s) was exposed. Five days after transfection, luciferase expression was determined. $^{*}p<0.01$ *vs.* pDNA with US. The Data are shown as mean±S.D. ($n=4$).

された（Fig. 6）．その発現は，少なくとも4週間は持続していた．さらにEGFPをコードした発現プラスミドを筋組織内に同様の方法で導入後，組織学的な発現解析を蛍光顕微鏡にて行ったところ，超音波照射エリアに依存した顕著なEGFP発現が確認できた（Fig. 7）．これらのことは，筋組織内に導入されたバブルリポソームが，超音波照射に応答して，効率よく崩壊し，それに伴うキャビテーション誘導を駆動力として遺伝子を細胞内へ送達させたものと考えられる．また，既存の遺伝子導入試薬として幅広く用いられているLipofectamin 2000（インビトロジェン社）では，ほとんど遺伝子導入活性が認められなかったことから，バブルリポソームの

in vivo での高い有用性が示された.

6. 動物モデルへの応用

次にわれわれは，バブルリポソームを利用した安全な超音波遺伝子デリバリーシステムの有用性を明らかとするために，疾患動物モデルへの応用を試みたので概説する.

6-1. 関節炎モデルマウスの遺伝子治療 Figure 5 及び 6 の結果に示されるようにバブルリポソームを利用する骨格筋への超音波遺伝子導入が効率よく達成されたことから，同様の導入条件（導入部位：脛部筋組織，超音波照射条件：1 MHz, 50% duty cycle, 60 s）にて，抗炎症性サイトカインとして知られている IL-10 遺伝子をコードしたプラスミド DNA をコラーゲン誘発性関節炎モデルマウスに対して，遺伝子治療を試み，その有用性を評価した. その結果，血清中での IL-10 タンパク質の発現分泌の上昇が，およそ 1 週間目で認められ，それは，3 週間ほどの持続性を示していた. さらに関節炎所見を観察し，スコア化したところ，顕著な関節炎の抑制が認められた（Fig. 8）. また，組織学的解析によっても，関節炎の進行に伴う関節破壊や滑膜肥厚の抑制が認められた. このことは，バブルリポソームによって，超音波遺伝子導入された筋組織から産

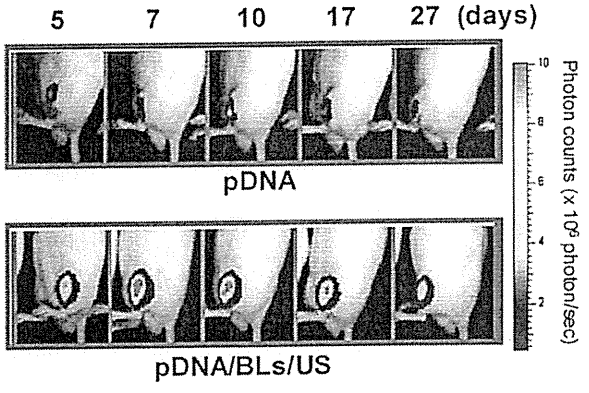

Fig. 6. *In vivo* Luciferase Imaging in Muscle Transfected with Bubble Liposomes and Ultrasound

Mice were treated with Bubble liposomes and ultrasound-mediated intramuscular luciferase gene transfer. After the transfection, *in vivo* luciferase expression was monitored at 0–27 days using an IVIS imaging system (Xenogen, CA, USA). pDNA (pCMV-Luciferase): 10 μg, Bubble liposomes: 30 μg, ultrasound exposure: (Frequency: 1 MHz, Duty: 50%, Intensity: 2 W/cm², Time: 60 s).

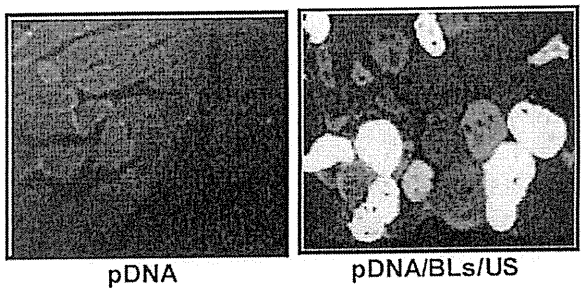

Fig. 7. EGFP Expression in Muscle Transfected with Bubble Liposomes and Ultrasound

Mice were treated with Bubble liposomes and ultrasound-mediated intramuscular EGFP gene transfer. After 5 days of transfection, the transfected muscle was sectioned and analyzed by fluorescent microscopy. pDNA (pEGFP-N3): 10 μg, Bubble liposomes: 30 μg, ultrasound exposure: (Frequency: 1 MHz, Duty: 50%, Intensity: 2 W/cm², Time: 60 s).

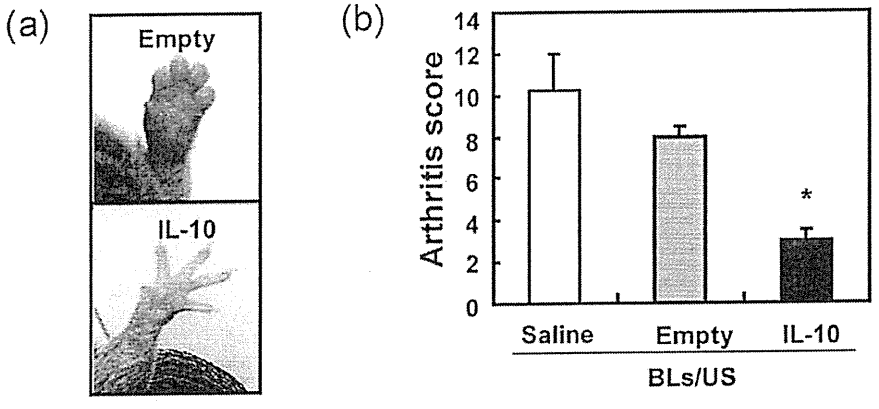

Fig. 8. Gene Transfer of IL-10 Plasmid into the Muscle of Collagen-induced Arthritis Model Mice by Bubble Liposomes and Ultrasound

Collagen-induced arthritis model mice were treated with Bubble liposomes and ultrasound-mediated intramuscular IL-10 gene transfer at days 21 after first immunization. (a) These photographs show the development of artritis in fore paw at days 49 after first immunization. (b) The development of artritis in fore and hind paws were counted. For example, score 1 or 2 indicates moderate symptom. In contrast, score 3 or 4 means severe arthritis. In the case of the treated group of IL-10 plasmid, the arthritis severity was significantly attenuated as compared with the treated group of saline or empty vector. $^{*}p<0.05$ *vs.* saline or empty vector. The data are shown as mean±S.D. ($n=10$).

生分泌されたIL-10タンパク質の全身循環作用によって，遠隔部位に存在する関節部位の炎症反応を効率的に沈静化したものと考えられる．よって，バブルリポソームによる安全な超音波遺伝子デリバリーシステムが，関節疾患への遺伝子治療法の一手段として有用であることが示された．同様の遺伝子導入法を用いて，下肢虚血モデルマウスに対する血管新生遺伝子治療を試みたところ，血管密度の増加や血流回復が観察されたことから，エンドクリン作用を期待するような局所筋組織の治療にも有用な遺伝子導入法となることも示している．

6-2. 腫瘍モデルマウスの遺伝子治療　骨格筋への遺伝子導入を利用したがん遺伝子治療を考える場合，効率よく骨格筋へ遺伝子導入し，タンパク質を産生させる必要がある．効率のよい遺伝子導入法として，骨格筋を支配する血管を介した遺伝子導入が，広範囲の遺伝子発現領域を確保できるため有効であると考えられる．しかし，血管と筋組織の間には，血管内皮細胞や筋内膜などの障壁が存在するため，これらの障壁を突破し，筋細胞内へと遺伝子導入する必要がある．これまでにわれわれは，血管を介した遺伝子デリバリーシステムとして，マウス下肢上部に止血帯を施し，大伏在静脈からpDNAとバブルリポソームの混合溶液を投与し，超音波照射を行うと組織透過性が増し，筋細胞内への遺伝子導入が可能となることを明らかとしてきた．[5] そこで，バブルリポソームと超音波併用による骨格筋への経静脈的遺伝子デリバリーシステムのがん遺伝子治療への可能性を探るべく治療用遺伝子を用いて，その有用性を評価した．今回，治療用遺伝子として，高い抗血管新生作用を持ち，臨床応用への可能性が期待されているplasminogen断片のkringle1–5をコードしたpDNAを用いた．Kringle1–5[13]は，既に抗血管新生タンパク質として知られているアンジオスタチンに相同性の高いKringle構造を有するタンパク質で，アンジオスタチンよりも50倍近い内皮細胞の増殖抑制効果を示すことから臨床応用が期待されている．そこでマウスメラノーマ由来B16細胞株をマウスの皮下に移植し，1週間後に骨格筋へ経静脈的に超音波遺伝子導入し，腫瘍増殖の抑制効果を観察した．その結果，バブルリポソームと超音波非照射群では腫瘍の増殖抑制効果が認められないのに対し，バブルリポソームと超音波照射併用群で，有意な腫瘍体積の抑制効果が認められた（Fig. 9）．また，同様の導入実験を簡便に新生血管を観察できるDorsal Air Sacモデルマウスに対して行った場合においても，がん細胞が誘発する背部皮下の新生血管の顕著な抑制が観察できた．よって，抗血管新生遺伝子治療におけるバブルリポソームを利用した経静脈的な骨格筋への超音波遺伝子デリバリーシステムの有用性が明らかとなった．

7. バブルリポソームを利用した骨格筋への超音波遺伝子デリバリーシステムの課題

ここまでバブルリポソームを利用する骨格筋への超音波遺伝子導入デリバリーシステムとその有用性を紹介してきたが，全身性疾患に対する遺伝子治療で必須なのは，広範囲で治療用遺伝子が導入発現することと安全性が確保されることである．本導入法は，広範囲の骨格筋で十分な活性が得られており，骨格筋で，生理活性タンパク質を発現分泌させるこ

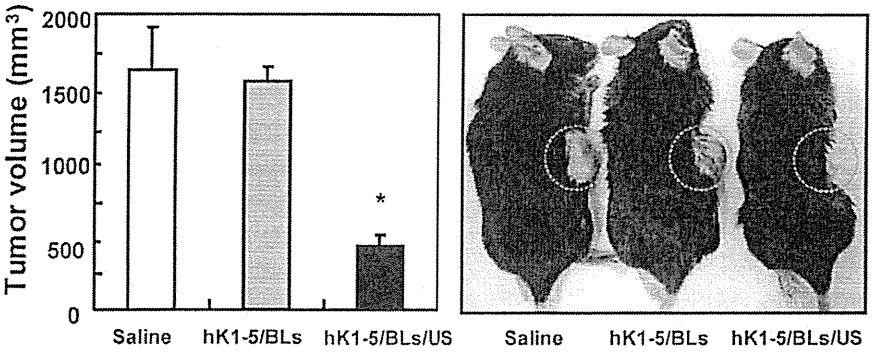

Fig. 9. Gene Transfer of hK1–5 Plasmid into the Muscle of Tumor Model Mice by Bubble Liposomes and Ultrasound

C57BL/6 mice were subcutaneously injected into right flank with B16. At 7 days after injection, when tumor volume become approximately 50 mm³, intravascular hK1–5 gene transfection into skeletal muscle by Bubble liposomes and ultrasound was performed. At 15 days, each tumor volume was measured. *$p<0.05$ *vs.* saline or empty vector. The data are shown as mean±S.D. ($n=6$).

とで全身循環作用を期待する疾患治療戦略の1つとして，その有用性を発揮できたものと考えられる．しかしながら，骨格筋を治療用タンパク質の供給源とすることは，疾患によっては，望まれない臓器や組織においても全身循環した生理活性タンパク質が作用し，それが重篤な副作用を引き起こす恐れも考えられる．例えば，今回のような抗炎症性サイトカインや抗血管新生タンパク質を用いた疾患治療においては，長期の全身作用によって，免疫力の低下を引き起こし，それが日和見感染症につながる恐れや虚血性疾患を誘発させてしまうことなども危惧される．

それゆえ，今後は，治療用タンパク質用の遺伝子発現ベクターを工夫することで発現量や発現時間をコントロールすることや産生分泌させるタンパク質に標的細胞への指向性を付与することで，安全かつ効率的なピンポイント治療が可能となると期待される．

8. おわりに

遺伝子工学が発展し，疾患関連遺伝子の発見や遺伝子診断技術の進歩に伴い，その情報を利用して治療を行う遺伝子治療への期待が高まっている．疾患の原因となる遺伝子の変異に対して，補完する遺伝子を導入したり，発現を抑えるアンチセンスを導入したりする方法が模索されている．しかし，いずれの場合においても，最適な導入技術が存在して初めて治療効果を獲得できる．そのような点で，バブルリポソームによる骨格筋への超音波遺伝子デリバリーシステムは，有用な手段と考えられる．今回紹介した関節炎やがん治療以外にも，上述の課題を克服することが可能となれば，感染症や循環器疾患などの治療にも適用範囲を拡大できるものと思われる．臨床応用に際しては，さらなる安全性の確保が求められるが，本研究成果が，その足掛かりとなることを期待したい．

謝辞　本稿で紹介した研究成果は，主に東京薬科大学薬学部薬物送達学教室と帝京大学薬学部生物薬剤学教室・丸山一雄先生，鈴木　亮先生との共同研究の一環として行われたものである．研究遂行にご協力頂いた当教室の学生諸子（特に福山哲也修士，角田由佳修士，関根祥子修士，松尾慶子修士，西島信明修士）に深謝する．また，本研究遂行にご協力頂いた昭和大学歯学部歯周病学教室・山本松男先生，東邦大学医療センター大森病院口腔外科・関谷秀樹先生，超音波照射に関する技術的なご指導を頂いた福岡大学医学部解剖学教室・立花克郎先生，ネッパジーン㈱・早川靖彦氏，鈴木孝尚氏に深謝する．さらに，本研究は独立行政法人新エネルギー・産業技術総合開発機構（NEDO）（Industrial Technology Research Grant Program (04A05010)），文科省科研費：萌芽研究（18650146），基盤研究(B)(20300179）の研究助成により遂行されたものであり，ここに深甚なる誠意を表します．

REFERENCES

1) Nishikawa M., Huang L., *Hum. Gene. Ther.*, **12**, 861–870 (2001).
2) Niidome N., Huang L., *Gene Ther.*, **9**, 1647–1652 (2002).
3) Suzuki R., Takizawa T., Negishi Y., Hagisawa K., Tanaka K., Sawamura K., Utoguchi N., Nishioka T., Maruyama K., *J. Control. Release*, **117**, 130–136 (2007).
4) Negishi Y., Endo Y., Fukuyama T., Suzuki R., Takizawa T., Omata D., Maruyama K., Aramaki Y., *J. Control. Release*, **132**, 124–130 (2008).
5) Negishi Y., Sekine S., Endo Y., Nishijima N., Suzuki R., Maruyama K., Aramaki Y., *AIP Conf. Proc.*, **1215**, 299–302 (2009).
6) Negishi Y., Omata D., Iijima H., Takabayashi Y., Suzuki K., Endo Y., Suzuki R., Maruyama K., Nomizu M., Aramaki Y., *Mol. Pharm.*, **7**, 217–226 (2010).
7) Suzuki R., Namai E., Oda Y., Nishiie N., Otake S., Koshima R., Hirata K., Taira Y., Utoguchi N., Negishi Y., *J. Control. Release*, **142**, 245–250 (2010).
8) Tachibana K., Tachibana S., *Jpn. J. Appl. Phys.*, **38**, 3014–3019 (1999).
9) Mitragotri S., *Nat. Rev. Drug Discov.*, **4**, 255–259 (2005).
10) Lawrie A., Brisken A. F., Francis S. E., Cumberland D. C., Crossman D. C., Newman C. M., *Gene Ther.*, **7**, 2023–2027 (2000).
11) Taniyama Y., Tachibana K., Hiraoka K., Namba T., Yamasaki K., Hashiya N., Aoki M., Ogihara T., Yasufumi K., Morishita R., *Circulation*, **105**, 1233–1239 (2002).

12) Maruyama K., Ishida O., Kasaoka S., Takizawa T., Utoguchi N., Shinohara A., Chiba M., Kobayashi H., Eriguchi M., Yanagie H., *J. Control. Release*, **98**, 195–207 (2004).
13) Cao R., Wu H. L., *Proc. Natl. Acad. Sci. USA*, **96**, 5728–5733 (1999).

Biomaterials 31 (2010) 7813–7826

Contents lists available at ScienceDirect

Biomaterials

journal homepage: www.elsevier.com/locate/biomaterials

Development of an ultrasound-responsive and mannose-modified gene carrier for DNA vaccine therapy

Keita Un [a,b], Shigeru Kawakami [a], Ryo Suzuki [c], Kazuo Maruyama [c], Fumiyoshi Yamashita [a], Mitsuru Hashida [a,d,*]

[a] Department of Drug Delivery Research, Graduate School of Pharmaceutical Sciences, Kyoto University, 46-29 Yoshida-shimoadachi-cho, Sakyo-ku, Kyoto 606-8501, Japan
[b] The Japan Society for the Promotion of Science (JSPS), Chiyoda-ku, Tokyo 102-8471, Japan
[c] Department of Biopharmaceutics, School of Pharmaceutical Sciences, Teikyo University, 1091-1 Suwarashi, Sagamiko, Sagamihara, Kanagawa 229-0195, Japan
[d] Institute for Integrated Cell-Material Sciences (iCeMS), Kyoto University, Yoshida-ushinomiya-cho, Sakyo-ku, Kyoto 606-8302, Japan

ARTICLE INFO

Article history:
Received 31 May 2010
Accepted 29 June 2010
Available online 24 July 2010

Keywords:
Gene transfer
Bubble lipoplexes
Ultrasound exposure
Mannose receptors
Antigen presenting cells
DNA vaccine therapy

ABSTRACT

Development of a gene delivery system to transfer the gene of interest selectively and efficiently into targeted cells is essential for achievement of sufficient therapeutic effects by gene therapy. Here, we succeeded in developing the gene transfection method using ultrasound (US)-responsive and mannose-modified gene carriers, named Man-PEG_{2000} bubble lipoplexes. Compared with the conventional lipofection method using mannose-modified carriers, this transfection method using Man-PEG_{2000} bubble lipoplexes and US exposure enabled approximately 500~800-fold higher gene expressions in the antigen presenting cells (APCs) selectively in vivo. This enhanced gene expression was contributed by the improvement of delivering efficiency of nucleic acids to the targeted organs, and by the increase of introducing efficiency of nucleic acids into the cytoplasm followed by US exposure. Moreover, high antitumor effects were demonstrated by applying this method to DNA vaccine therapy using ovalbumin (OVA)-expressing plasmid DNA (pDNA). This US-responsive and cell-specific gene delivery system can be widely applied to medical treatments such as vaccine therapy and anti-inflammation therapy, which its targeted cells are APCs, and our findings may help in establishing innovative methods for in-vivo gene delivery to overcome the poor introducing efficiency of carriers into cytoplasm which the major obstacle associated with gene delivery by non-viral carriers.

1. Introduction

In the post-genome era, the analysis of disease-related genes has rapidly advanced, and the medical application of the information obtained from gene analysis is being put into practice. In particular, the development of effective method to transfer the gene of interest selectively and efficiently into the targeted cells is essential for the gene therapy of refractory diseases, in-vivo functional analysis of genes and establishment of animal models for diseases. However, a suitable carrier for selective and efficient gene transfer to the targeted cells is still being developed. Although various types of viral and non-viral carriers have been developed for gene transfer, they are limited to use by viral-associated pathogenesis and low transfection efficiency, respectively. For the cell-selective gene transfer, many investigators have focused on ligand-modified non-viral carriers such as liposomes [1–4], emulsions [5], micelles [6] and polymers [7], because of their high productivity and low toxicity. On the other hand, since the gene transfection efficiency by non-viral carriers is poor, it is difficult to obtain the effective therapeutic effects by gene therapy using non-viral carriers. Moreover, in the gene transfection using conventional ligand-modified non-viral carriers, since the carriers need to be taken up into cells via endocytosis following by interaction with targeted molecules on the cell membrane, the number of candidates which are suitable as ligands for targeted gene delivery is limited.

Some researchers have attempted to develop the transfection method using external stimulation, such as electrical energy [8], physical pressure [9] and water pressure [10], to enhance the gene transfection efficiency. Among these, gene transfection method using US exposure and microbubbles enclosing US imaging gas, called "sonoporation method", have been focused as effective drug/gene delivery systems [11–14]. In the sonoporation method, microbubbles are degraded by US exposure with optimized intensity, then cavitation energy is generated by the destruction of

* Corresponding author. Department of Drug Delivery Research, Graduate School of Pharmaceutical Sciences, Kyoto University, 46-29 Yoshida-shimoadachi-cho, Sakyo-ku, Kyoto 606-8501, Japan. Tel.: +81 75 753 4545; fax: +81 75 753 4575.
E-mail address: hashidam@pharm.kyoto-u.ac.jp (M. Hashida).

0142-9612/$ – see front matter © 2010 Elsevier Ltd. All rights reserved.
doi:10.1016/j.biomaterials.2010.06.058

microbubbles. Consequently, the transient pores are created on the cell membrane, and large amount of nucleic acids are directly introduced into the cytoplasm through the created pores [13,15,16]. However, the in-vivo gene transfection efficiency by conventional sonoporation method administering the nucleic acids and microbubbles separately is low because of the rapid degradation of nucleic acids in the body [17], the large particle size of conventional microbubbles [15] and the different pharmacokinetic profiles of the nucleic acids and microbubbles. Moreover, to transfer the gene into the targeted cells selectively by sonoporation method in vivo, the control of in-vivo distribution of nucleic acids and microbubbles, which are separately administered, is necessary.

In our previous report [16], we have demonstrated the effective transfection by combination-use method using our mannosylated lipoplexes composed of Man-C4-chol: DOPE [1], and conventional Bubble liposomes (BLs) [12] with US exposure. However, this combination-use method is complicated because of the necessity for multiple injections of mannosylated lipoplexes and BLs; therefore, it is difficult to apply for medical treatments using multiple transfections. In addition, the difference of in-vivo distribution characteristics between mannosylated lipoplexes and BLs might be decreased its transfection efficacy. Therefore, it is essential to develop the US-responsive and cell-selective gene carriers constructed with ligand-modified gene carriers and microbubbles.

Taking these into considerations, we examined the gene transfection system for effective DNA vaccine therapy using physical stimulation and ligand-modification. First, we developed US-responsive and mannose-modified gene carriers, Man-PEG_{2000} bubble lipoplexes (Fig. 1), by enclosing perfluoropropane gas into mannose-conjugated PEG_{2000}-DSPE-modified cationic liposomes (DSTAP: DSPC: Man-PEG_{2000}-DSPE (Fig. 1))/pDNA complexes. Then, we evaluated the enhanced and cell-selective gene expression in the APCs by intravenous administration of Man-PEG_{2000} bubble lipoplexes and external US exposure in mice. Finally, we examined high anti-tumor effects by applying this method to DNA vaccine therapy using OVA-expressing pDNA.

2. Materials and methods

2.1. Mice and cell lines

Female ICR mice (4~5 weeks old) and C57BL/6 mice (6~8 weeks old) were purchased from the Shizuoka Agricultural Cooperative Association for Laboratory Animals (Shizuoka, Japan). All animal experiments were carried out in accordance with the Principles of Laboratory Animal Care as adopted and promulgated by the US National Institutes of Health and the guideline for animal experiments of Kyoto University. CD8-OVA1.3 cells, T cell hybridomas with specificity for OVA 257~264-kb, were kindly provided by Dr. C.V. Harding (Case Western Reserve University, Cleveland, OH, USA) [18]. EL4 cells (C57BL/6 T-lymphomas) and E.G7-OVA cells (the OVA-transfected clones of EL4) were purchased from American Type Culture Collection (Manassas, VA). CD8-OVA1.3 cells and EL4 cells were maintained in Dulbecco's modified Eagle's medium and E.G7-OVA cells were maintained in RPMI-1640. Both mediums were supplemented with 10% fetal bovine serum (FBS), 0.05 mM 2-mercaptoethanol, 100 IU/mL penicillin, 100 μg/mL streptomycin and 2 mM L-glutamine at 37 °C in 5% CO_2.

2.2. pDNA

pCMV-Luc and pCMV-OVA were constructed in our previous reports [19,20]. Briefly, pCMV-Luc was constructed by subcloning the HindIII/Xba I firefly luciferase cDNA fragment from pGL3-control vector (Promega, Madison, WI, USA) into the polylinker of pcDNA3 vector (Invitrogen, Carlsbad, CA, USA). pCMV-OVA was constructed by subcloning the EcoRI chicken egg albumin (ovalbumin) cDNA fragment from pAc-neo-OVA, which was kindly provided by Dr. M.J. Bevan (University of Washington, Seattle, WA, USA) into the polylinker of pVAX I. pDNA were amplified in the E. coli strain DH5α, isolated and purified using a QIAGEN Endofree Plasmid Giga Kit (QIAGEN GmbH, Hilden, Germany).

2.3. Synthesis of Man-PEG_{2000}-DSPE and preparation of Man-PEG_{2000} bubble lipoplexes

Man-PEG_{2000}-DSPE was synthesized in a one-step reaction by covalent binding with NH_2-PEG_{2000}-DSPE (NOF Co., Tokyo, Japan) and 2-imino-2-methoxyethyl-1-thiomannoside (IME-thiomannoside). IME-thiomannoside was prepared according to the method of Lee [21]. Next, NH_2-PEG_{2000}-DSPE and IME-thiomannoside were reacted, vacuum dried and dialyzed to produce Man-PEG_{2000}-DSPE, and then, the resultant dialysates were lyophilized. To produce the liposomes for bubble lipoplexes, DSTAP (Avanti Polar Lipids Inc., Alabaster, AL, USA), DSPC (Sigma Chemicals Inc., St. Louis, MO, USA) and Man-PEG_{2000}-DSPE or NH_2-PEG_{2000}-DSPE were mixed in chloroform at a molar ratio of 7:2:1. For construction of BLs, DSPC and methoxy-PEG_{2000}-DSPE (NOF Co., Tokyo, Japan) were mixed in chloroform at a molar ratio of 94:6. The mixture for the construction of liposomes was dried by evaporation, vacuum desiccated and the resultant lipid film was resuspended in sterile 5% dextrose. After hydration for 30 min at 65 °C, the dispersion was sonicated for 10 min in a bath sonicator and for 3 min in a tip sonicator to produce liposomes. Then, liposomes were sterilized by passage through a 0.45 μm filter (Nihon-Millipore, Tokyo, Japan). The lipoplexes were prepared by gently mixing with equal volumes of pDNA and liposome solution at a charge ratio of 1.0:2.3 (−:+). For preparation of BLs and bubble lipoplexes, the enclosure of US imaging gas into liposomes and lipoplexes was performed according to our previous report [16]. Briefly, prepared liposomes and lipoplexes were added to 5 mL sterilized vials, filled with perfluoropropane gas (Takachiho Chemical Industries Co., Ltd., Tokyo, Japan), capped and then pressured with 7.5 mL of perfluoropropane gas. To enclose US imaging gas into the liposomes and lipoplexes, the vial was sonicated using a bath-type sonicator (AS ONE Co., Osaka, Japan) for 5 min. The particle sizes and zeta

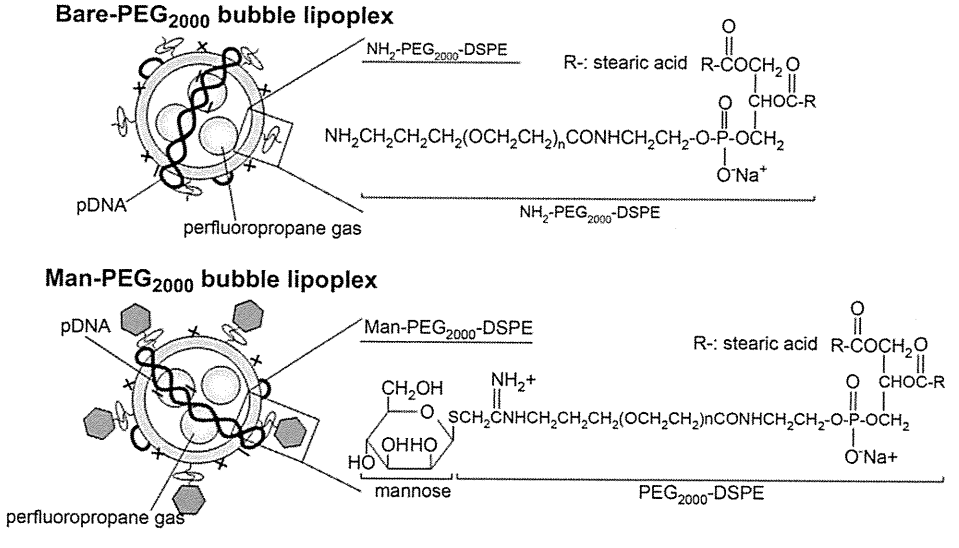

Fig. 1. Structure of Bare-PEG_{2000} bubble lipoplex containing NH_2-PEG_{2000}-DSPE and Man-PEG_{2000} bubble lipoplex containing Man-PEG_{2000}-DSPE used in this study.

potentials of liposomes and lipoplexes were determined by a Zetasizer Nano ZS instrument (Malvern Instrument, Ltd., Worcestershire, UK).

2.4. Harvesting of mouse peritoneal macrophages

Mouse peritoneal macrophages were harvested and cultured according to our previous report [16]. Briefly, the macrophages were harvested from mice at 4 days after intraperitoneal injection of 2.9% thioglycolate medium (1 mL). The collected macrophages were washed and suspended in RPMI-1640 medium supplemented with 10% FBS, 100 IU/mL penicillin, 100 μg/mL streptomycin and 2 mM L-glutamine, and plated on culture plates. After incubation for 2 h at 37 °C in 5% CO_2, non-adherent cells were washed off with culture medium, and the macrophages were incubated for another 72 h.

2.5. In-vitro gene transfection

After the macrophages were collected and incubated for 72 h, the culture medium was replaced with Opti-MEM I containing bubble lipoplexes (5 μg pDNA). The macrophages were exposed to US (frequency, 2.062 MHz; duty, 50%; burst rate, 10 Hz; intensity 4.0 W/cm^2) for 20 s using a 6 mm diameter probe placed in the well at 5 min after addition of bubble lipoplexes. In the transfection using naked pDNA and BLs, at 5 min after addition of naked pDNA (5 μg) and BLs (60 μg total lipids) were added, and the macrophages were immediately exposed to US. US was generated using a Sonopore-4000 sonicator (NEPA GENE, Chiba, Japan). Then, 1 h later, the incubation medium was replaced with RPMI-1640 and incubated for an additional 23 h. Lipofectamine® 2000 (Invitrogen, Carlsbad, CA, USA) was used according to the recommended procedures, and the exposure time of Lipofectamine® 2000 was 1 h, which is the same exposure time in other experiments using lipoplexes. Following incubation for 24 h, the cells were scraped from the plates and suspended in lysis buffer (0.05% Triton X-100, 2 mM EDTA, 0.1 M Tris, pH 7.8). Then, the cell suspension was shaken, and centrifuged at 10,000g, 4 °C for 10 min. The supernatant was mixed with luciferase assay buffer (Picagene, Toyo Ink Co., Ltd., Tokyo, Japan) and the luciferase activity was measured in a luminometer (Lumat LB 9507, EG&G Berthold, Bad Wildbad, Germany). The luciferase activity was normalized with respect to the protein content of cells. The protein concentration was determined with a Protein Quantification Kit (Dojindo Molecular Technologies, Inc., Tokyo, Japan). The level of luciferase mRNA expression was determined by RT-PCR.

2.6. Inhibitory experiments of endocytosis in vitro

Endocytosis was inhibited by chlorpromazine (50 μM) as clathrin-mediated endocytosis inhibitor [22], genistein (200 μM) as caveolae-mediated endocytosis inhibitor [23] and 5-(*N*-ethyl-*N*-isopropyl)amiloride (EIPA, 50 μM) as macropinocytosis inhibitor [24]. Each endocytosis inhibitor was added to the macrophages at 30 min before the addition of lipoplexes.

2.7. Fluorescence photographs of pDNA in mouse peritoneal macrophages

To visualize the cellular association of pDNA by fluorescence microscopy (Biozero BZ-8000, KEYENCE, Osaka, Japan), lipoplexes were constructed with TM-rhodamine-labeled pDNA prepared by a Label IT Nucleic Acid Labeling Kit (Mirus Co., Madison, WI, USA).

2.8. Evaluation of cytotoxic effects by MTT assay

The cytotoxicity was evaluated by MTT assay. Briefly, 3-(4,5-dimethyl-2-thiazol)-2,5-diphenyltetrazolium bromide (MTT, Nacalai Tesque, Inc., Kyoto, Japan) solution was added to each well and incubated for 4 h. The resultant formazan crystals were dissolved in 0.04 M HCl-isopropanol and sonicated for 10 min in a bath sonicator. Absorbance values at 550 nm (test wavelength) and 655 nm (reference wavelength) were measured and the results were expressed as viability (%).

2.9. In-vivo gene transfection

Four-week-old ICR female mice were intravenously injected with 400 μL bubble lipoplexes via the tail vein using a 26-gauge syringe needle at a dose of 50 μg pDNA. At 5 min after the injection of bubble lipoplexes, US (frequency, 1.045 MHz; duty, 50%; burst rate, 10 Hz; intensity 1.0 W/cm^2; time, 2 min) was exposed transdermally to the abdominal area using a Sonopore-4000 sonicator with a probe of diameter 20 mm. In the transfection using naked pDNA and BLs, at 4 min after intravenous injection of BLs (500 μg total lipid), naked pDNA (50 μg) was intravenously injected and US was exposed at 1 min after naked pDNA injection. At predetermined times after injection, mice were sacrificed and their organs collected for each experiment. The organs were washed twice with cold saline and homogenized with lysis buffer (0.05% Triton X-100, 2 mM EDTA, 0.1 M Tris, pH 7.8). The lysis buffer was added in a weight ratio of 5 mL/g for the liver or 4 mL/g for the other organs. After three cycles of freezing and thawing, the homogenates were centrifuged at 10,000g, 4 °C for 10 min. The luciferase activity of resultant supernatant was determined by luciferase assay and the level of luciferase mRNA expression was determined by RT-PCR.

2.10. In-vivo imaging

At 6 h after transfection, anesthetized mice were administrated D-luciferin (10 mg/300 μL PBS) (Promega Co., Madison, WI, USA). At 10 min after injection of D-luciferin, organs were excised and luminescent images were taken by NightOWL LB 981 NC instrument (Berthold Technologies, GmbH, Bad Wildbad, Germany). The pseudocolor luminescent images were generated, overlaid with organ images and the luminescence representation was obtained using WinLight software (Berthold Technologies GmbH, Bad Wildbad, Germany).

2.11. Separation of mouse hepatic PCs and NPCs

The separation of mouse hepatic PCs and NPCs was performed according to our previous reports [19]. Briefly, at 6 h after in-vivo transfection using bubble lipoplexes and US exposure, each mouse was anesthetized with pentobarbital sodium (40~60 mg/kg) and the liver was perfused with perfusion buffer (Ca^{2+}, Mg^{2+}-free HEPES solution, pH 7.2) for 10 min. Then, the liver was perfused with collagenase buffer (HEPES solution, pH 7.5 containing 5 mM $CaCl_2$ and 0.05% (w/v) collagenase (type I)) for 5 min. Immediately after the start of perfusion, the vena cava and aorta were cut and the perfusion rate was maintained at 5 mL/min. At the end of perfusion, the liver was excised. The cells were dispersed in ice-cold Hank's-HEPES buffer by gentle stirring and then filtered through cotton mesh sieves, followed by centrifugation at 50g for 1 min. The pellets containing the hepatic PCs were washed five times with Hank's-HEPES buffer by centrifuging at 50g for 1 min. The supernatant containing the hepatic NPCs was similarly centrifuged 5 times and the resulting supernatant was centrifuged twice at 300g for 10 min. Then, the PCs and NPCs were resuspended separately in ice-cold Hank's-HEPES buffer.

2.12. Isolation of mouse splenic CD11c$^+$ cells

The isolation of mouse splenic CD11c$^+$ cells was performed according to our previous reports [25]. Briefly, At 6 h after in-vivo transfection using bubble lipoplexes and US exposure, the splenic cells were suspended in ice-cold RPMI-1640 medium on ice. Red blood cells were removed by incubation with hemolytic reagent (0.15 M NH_4Cl, 10 mM $KHCO_3$, 0.1 mM EDTA) for 3 min at room temperature. The CD11c$^+$ cells were isolated by magnetic cell sorting with anti-mouse CD11c (N418) microbeads and auto MACS (Miltenyi Biotec, Inc., Auburn, CA, USA) following the manufacturer's instructions.

2.13. Quantitative RT-PCR

Total RNA was isolated from separated cells using a GenElute Mammalian Total RNA Miniprep Kit (Sigma-Aldrich, St. Louis, MO, USA). Reverse transcription of mRNA was carried out using a PrimeScript® RT reagent Kit (Takara Bio Inc., Shiga, Japan). Real-time PCR was performed using SYBR® Premix Ex Taq (Takara Bio Inc., Shiga, Japan) and Lightcycler Quick System 350S (Roche Diagnostics, Indianapolis, IN, USA) with primers. The primers for luciferase and gapdh cDNA were constructed as follows: primer for luciferase cDNA, 5′-TTCTTCGCCAAAAGCACTC-3′ (forward) and 5′-CCCTCGGGTGTAATCAGAAT-3′ (reverse); primer for gapdh, 5′-TCTCCTGCGACTTCAACA-3′ (forward) and 5′-GCTGTAGCCGTATTCATTGT-3′ (reverse) (Sigma-Aldrich, St. Louis, MO, USA). The mRNA copy numbers were calculated for each sample from the standard curve using the instrument software ('Arithmetic Fit Point analysis' for the Lightcycler). The results were expressed as the ratio of luciferase mRNA copy numbers to the housekeeping gene (gapdh) mRNA copy numbers.

2.14. Tissue distribution of radio-labeled pDNA

Lipoplexes constructed with ^{32}P-labeled pDNA ([α-^{32}P]-dCTP, PerkinElmer, Inc., MA, USA) [26] were injected intravenously into mice. At predetermined times after injection, blood was collected from the vena cava under pentobarbital anesthesia. Then, mice were sacrificed and the organs were collected, rinsed with saline and weighed. The tissues were dissolved in Soluene-350 and the resultant lysates were decolorized with isopropanol and 30% H_2O_2, and then neutralized with 5 N HCl. The radioactivity of ^{32}P-labeled pDNA was measured in scintillation counter (LSA-500, Beckman Coulter, Inc., CA, USA) after addition of Clear-Sol I solution.

2.15. Measurement of transaminase activity in the serum

At predetermined times after transfection, the serum was collected from the anesthetized mice. Alanine aminotransferase (ALT) and aspartate aminotransferase (AST) activities in the serum were determined using Transaminase CII-Test Wako kit (Wako Pure Chemical Industries Ltd., Tokyo, Japan) according to manufacturer's instructions.

2.16. Antigen presenting assay

The evaluation of antigen presentation on MHC class I molecules in the splenic dendritic cells was performed by in-vitro antigen presentation assay using CD8-OVA1.3 cells, which are T cell hybridomas with specificity for OVA. The $CD11c^+$ cells isolated from immunized mice were plated in a 96-well plate at various cells numbers and co-cultured with CD8-OVA1.3 cells (1×10^5) for 20 h. The antigen presentation on MHC class I molecules was evaluated by IL-2 secreted from activated CD8-OVA1.3 cells measured by a commercial IL-2 ELISA Kit (Bay bioscience Co., Ltd., Hyogo, Japan).

2.17. Evaluation of OVA-specific cytokine secretion from the splenic cells

At 2 weeks after the last immunization, the splenic cells collected from immunized mice were plated in 96-well plates and incubated for predetermined times at 37 °C in the presence or absence of OVA (100 μg). IFN-γ and IL-4 in the culture medium were measured by the commercial ELISA Kit, respectively (Bay bioscience Co., Ltd., Hyogo, Japan).

2.18. OVA-specific CTL assay

At 2 weeks after the last immunization, the splenic cells harvested from immunized mice were plated in 6-well plates and co-incubated with mitomycin C-treated E.G7-OVA cells or EL4 cells for 4 days. After co-incubation, non-adherent cells were collected, washed and plated in 96-well plates with target cells (E.G7-OVA cells or EL4 cells) at various effector/target (E/T) ratios. The target cells were labeled with ^{51}Cr by incubating with $Na_2^{51}CrO_4$ (PerkinElmer, Inc., MA, USA) in culture medium for 1 h at 37 °C. At 4 h after incubation, the plates were centrifuged and the resultant supernatant of each well was collected and the radioactivity of released ^{51}Cr was measured in a gamma counter. The percentage of ^{51}Cr release was calculated as follows: specific (lysis (%) = [(experimental ^{51}Cr release − spontaneous ^{51}Cr release)/(maximum ^{51}Cr release − spontaneous ^{51}Cr release)] × 100). The percentage of OVA-specific ^{51}Cr release was calculated as (% of ^{51}Cr release from E.G7-OVA cells) − (% of ^{51}Cr release from EL4 cells).

2.19. Therapeutic effects

C57BL/6 mice were immunized three times biweekly. At 2 weeks after last immunization, E.G7-OVA cells and EL4 cells were transplanted subcutaneously into the back of mice. The tumor growth and survival of mice were monitored up to 80 days after transplantation of E.G7-OVA cells and EL4 cells.

2.20. Statistics

Results were presented as the mean ± SD of more than three experiments. Analysis of variance (ANOVA) was used to test the statistical significance of differences among groups. Two-group comparisons were performed by the Student's *t*-test. Multiple comparisons between control groups and other groups were performed by the Dunnett's test and multiple comparisons between all groups were performed by the Tukey-Kramer test.

3. Results

3.1. In-vitro gene transfection properties by Man-PEG_{2000} lipoplexes

Polyethylene-glycol (PEG) modification of particles is necessary to enclose US imaging gas stably and to prepare the

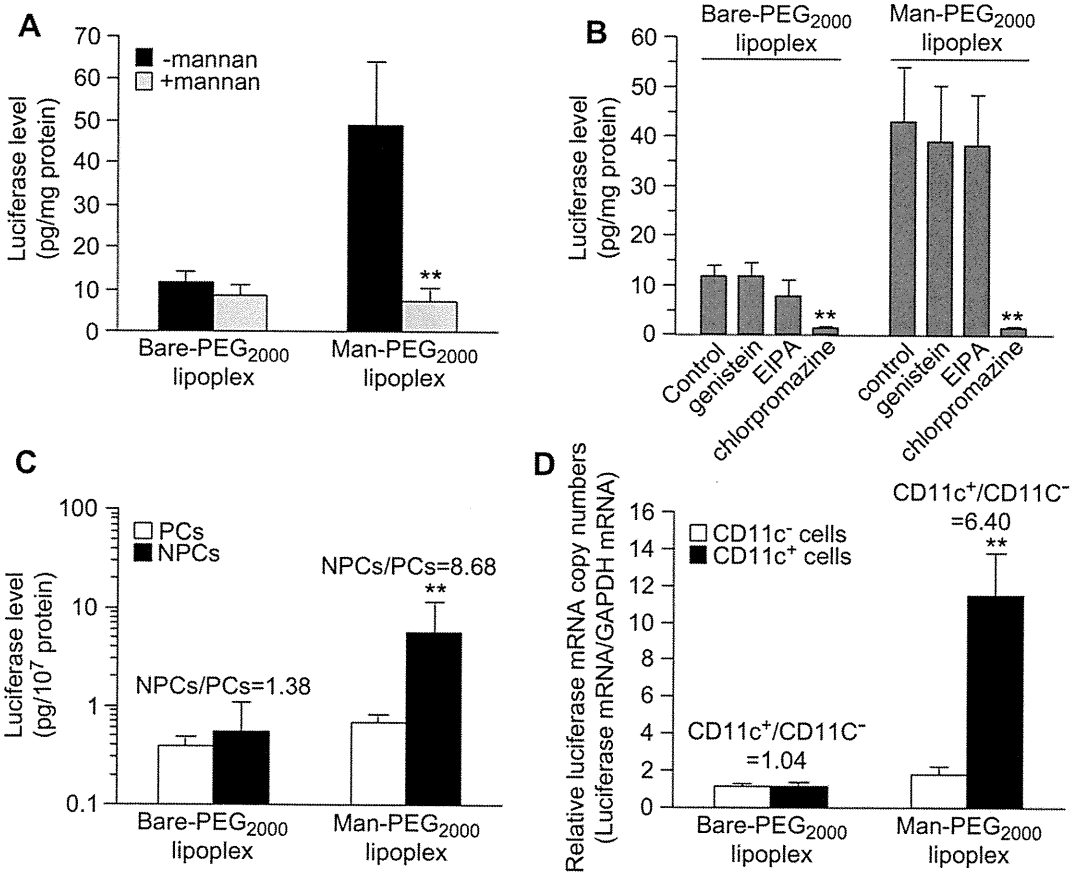

Fig. 2. The mannose receptor-expressing cell-selective gene expression by Man-PEG_{2000} lipoplexes containing Man-PEG_{2000} lipids in vitro and vivo. (A) The level of luciferase expression obtained by Bare-PEG_{2000} lipoplexes and Man-PEG_{2000} lipoplexes (5 μg pDNA) in the absence or presence of 1 mg/mL mannan in mouse cultured macrophages at 24 h after transfection. $^{**}p < 0.01$, compared with the corresponding group of mannan. (B) Inhibition of luciferase expression obtained by Bare-PEG_{2000} lipoplexes and Man-PEG_{2000} lipoplexes (5 μg pDNA) in addition of various endocytosis inhibitors in mouse cultured macrophages at 24 h after transfection. $^{**}p < 0.01$, compared with the corresponding group of control. (C) The level of luciferase expression in mouse hepatic PCs and NPCs after intravenous administration of Bare-PEG_{2000} lipoplexes and Man-PEG_{2000} lipoplexes (50 μg pDNA) in mice at 6 h after transfection. $^{**}p < 0.01$, compared with the corresponding group of PCs. (D) The level of luciferase mRNA expression in mouse splenic $CD11c^+$ cells and $CD11c^-$ cells after intravenous administration of Bare-PEG_{2000} lipoplexes and Man-PEG_{2000} lipoplexes (50 μg pDNA) in mice at 6 h after transfection. $^{**}p < 0.01$, compared with the corresponding group of $CD11c^-$ cells. Each value represents the mean + SD ($n = 3–4$).

small-sized microbubbles for in-vivo administration [12]. Firstly, we developed mannose-conjugated PEG_{2000}-modified lipids (Man-PEG_{2000}-DSPE (Fig. 1)) to prepare the APC-targeted small-sized microbubbles and determined the in-vitro and in-vivo transfection characteristics of mannose-conjugated PEG_{2000}-modified lipoplexes (Man-PEG_{2000} lipoplexes) containing Man-PEG_{2000} lipids. The particle sizes and zeta potentials of Man-PEG_{2000} lipoplexes and non-modified PEG_{2000}-lipoplexes (Bare-PEG_{2000} lipoplexes) were approximately 150 nm and +40 mV, respectively (Supplementary Table 1). In mouse cultured macrophages expressing mannose receptors abundantly, the level of gene expression obtained by Man-PEG_{2000} lipoplexes were significantly higher than those by Bare-PEG_{2000} lipoplexes (Fig. 2A and B). Then, the level of gene expression obtained by Man-PEG_{2000} lipoplexes was suppressed to same extent as that by Bare-PEG_{2000} lipoplexes in the presence of an excess of mannan (Fig. 2A). Moreover, this level of gene expression obtained by Man-PEG_{2000} lipoplexes was also suppressed to same extent as that by Bare-PEG_{2000} lipoplexes in the presence of chlorpromazine (Fig. 2B), which is the inhibitor of clathrin-mediated endocytosis [22]. These results agreed with the results of cellular association of pDNA (Supplementary Fig. 1), and suggest that Man-PEG_{2000} lipoplexes are taken up into the cells via clathrin-mediated endocytosis following the interaction with mannose receptors.

3.2. In-vivo gene transfection properties by Man-PEG_{2000} lipoplexes

Since the degradation of pDNA by nuclease in the blood is one of the critical factors in the in-vivo gene transfection by intravenously administration of lipoplexes, we investigated the stability of Bare-PEG_{2000} lipoplexes and Man-PEG_{2000} lipoplexes against nucleases. Following electrophoresis of naked pDNA and lipoplexes after incubation with DNase I, although naked pDNA underwent the degradation by DNase I, lipoplexes did not undergo the degradation and retained the complex forms (Supplementary Fig. 2). Then, we investigated the gene expression characteristics of Man-PEG_{2000} lipoplexes in the liver and spleen, which are the targeted organs of mannose-modified carriers [27]. In this study, liver was separated in the parenchymal cells (PCs) and non-parenchymal cells (NPCs), and spleen was separated in the dendritic cells ($CD11c^+$ cells) and other cells ($CD11c^-$ cells). As shown in Fig. 2C and D, following intravenous administration of Man-PEG_{2000} lipoplexes, selective gene expression was observed in the hepatic NPCs and the splenic $CD11c^+$ cells, which are the APCs expressing mannose receptors abundantly [28–30].

3.3. In-vitro gene transfection efficiency by Man-PEG_{2000} bubble lipoplexes and US exposure

Although Man-lipoplexes showed the APC-selective gene transfection properties in vivo, this level of gene expression was

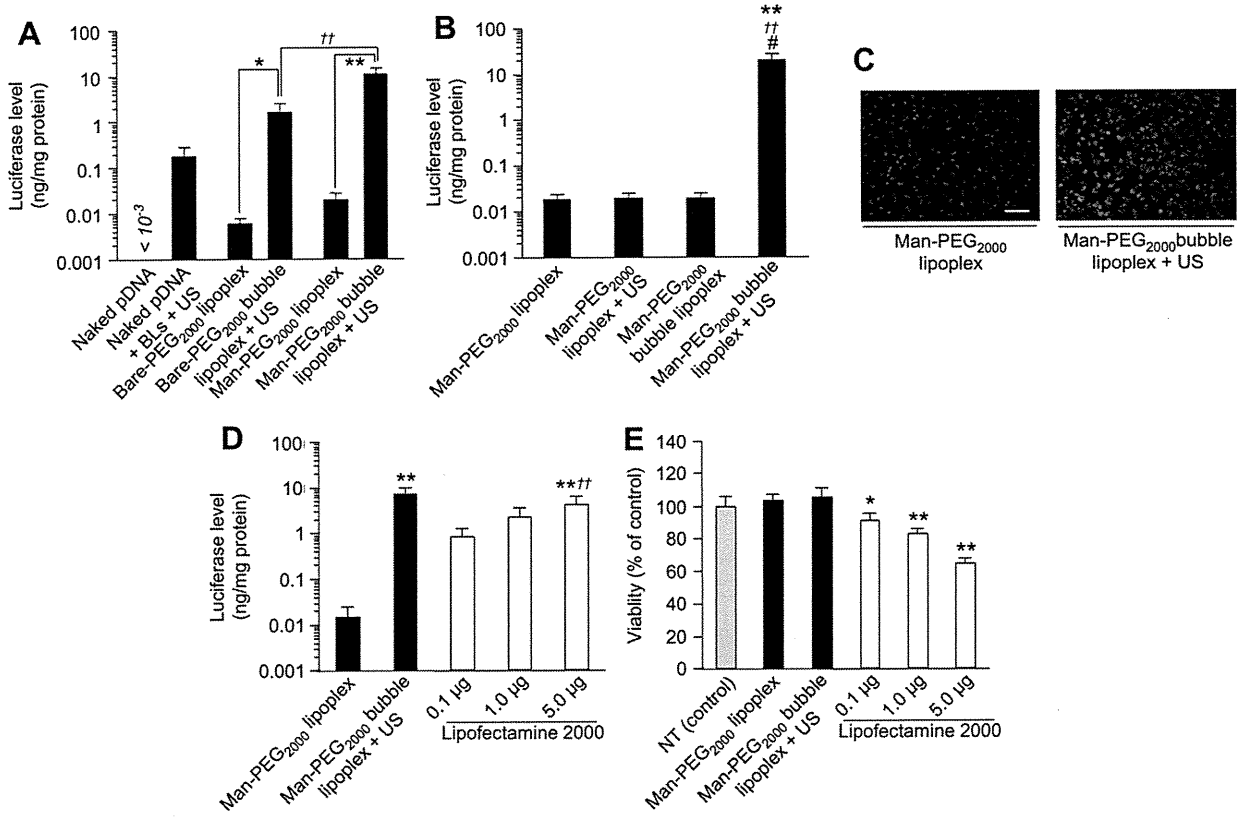

Fig. 3. Enhancement of gene expression by Man-PEG_{2000} bubble lipoplexes and US exposure in vitro. (A) The level of luciferase expression obtained by naked pDNA, naked pDNA + BLs with US exposure, Bare-PEG_{2000} lipoplexes, Bare-PEG_{2000} bubble lipoplexes with US exposure, Man-PEG_{2000} lipoplexes and Man-PEG_{2000} bubble lipoplexes with US exposure (5 μg pDNA) at 24 h after transfection. Significant difference; $^*p < 0.05$; **, $^{††}p < 0.01$. (B) The level of luciferase expression obtained by Man-PEG_{2000} lipoplexes and Man-PEG_{2000} bubble lipoplexes with or without US exposure (5 μg pDNA) at 24 h after transfection. $^{**}p < 0.01$, compared with Man-PEG_{2000} lipoplex, $^{††}p < 0.01$, compared with Man-PEG_{2000} lipoplex + US, $^{‡‡}p < 0.01$, compared with Man-PEG_{2000} bubble lipoplex. (C) Representative fluorescent images of cellular association of pDNA obtained by Man-PEG_{2000} lipoplexes and Man-PEG_{2000} bubble lipoplexes with US exposure (5 μg pDNA) at 2 h after treatment. Lipoplexes were constructed with TM-rhodamine-labeled pDNA. TM-rhodamine-labeled pDNA (red), nuclei counterstained by DAPI (blue). Scale bars, 100 μm. (D) Comparison of the level of luciferase expression obtained by Man-PEG_{2000} bubble lipoplexes (5 μg pDNA) and US exposure with that by Lipofectamine 2000. $^{**}p < 0.01$, compared with Man-PEG_{2000} lipoplexes, $^{††}p < 0.01$, compared with Lipofectamine 2000 (0.1 μg). (E) Comparison of cell viability by transfection using Man-PEG_{2000} bubble lipoplexes (5 μg pDNA) and US exposure with that by Lipofectamine 2000. N.T., non-treatment. $^*p < 0.05$; $^{**}p < 0.01$, compared with N.T. Each value represents the mean + SD ($n = 4$).

low compared with our previous reports [1,19,25]. To enhance the level of gene expression by sonoporation method, we developed Man-PEG_{2000} bubble lipoplexes (Fig. 1) by enclosing US imaging gas (perfluoropropane gas) into Man-PEG_{2000} lipoplexes. The lipid composition of lipoplexes is important for the stable enclosure of US imaging gas. Following optimization of lipid composition, lipoplexes constructed with the saturated lipids only, which have a high melting temperature (T_m), were enclosed US imaging gas stably (Supplementary Table 2). Following enclosure of US imaging gas in lipoplexes, lipoplexes became cloudy and their particle sizes were increased (from 150 nm to 550 nm, approximately) (Supplementary Fig. 3A and Table 3). Then, since the zeta potentials of bubble lipoplexes were lower than that of bubble liposomes and same as that of lipoplexes (Supplementary Tables 1 and 3), it is considered that pDNA is attached on the surface of bubble liposomes. Moreover, the stability against nucleases observed in Man-PEG_{2000} lipoplexes (Supplementary Fig. 2) was maintained after enclosure of US imaging gas into lipoplexes (Supplementary Fig. 3B).

The level of gene expression obtained by Man-PEG_{2000} bubble lipoplexes and US exposure was 500-fold higher than that by Man-PEG_{2000} lipoplexes in mouse cultured macrophages expressing mannose receptors abundantly, and also higher than that by non-modified bubble lipoplexes (Bare-PEG_{2000} bubble lipoplexes, Fig. 1) and US exposure or conventional sonoporation method using naked pDNA and BLs (Fig. 3A). This enhanced gene expression was observed when bubble lipoplexes and US exposure were used for in-vitro gene transfer (Fig. 3B). The cellular association of pDNA obtained by transfection using Man-PEG_{2000} bubble lipoplexes and US exposure was also 10-fold higher than that by Man-PEG_{2000} lipoplexes, and also higher than that by Bare-PEG_{2000} bubble lipoplexes and US exposure or conventional sonoporation method using naked pDNA and BLs (Fig. 3C and Supplementary Fig. 4A). Moreover, this level of gene expression obtained by Man-PEG_{2000} bubble lipoplexes and US exposure was comparable to that by Lipofectamine® 2000, which is widely used as a gene transfection reagent (Fig. 3D). On the other hand, the cytotoxicity by Man-PEG_{2000} bubble lipoplexes and US exposure was lower than that by Lipofectamine® 2000 (Fig. 3E).

3.4. Intracellular uptake properties of pDNA by Man-PEG_{2000} bubble lipoplexes and US exposure

The gene expression obtained by Man-PEG_{2000} bubble lipoplexes and US exposure was significantly suppressed in the presence of an excess of mannan (Fig. 4A). Therefore, the interaction with mannose receptors on the cell membrane is involved in the gene transfection by Man-PEG_{2000} bubble lipoplexes and US exposure, similar to the gene transfection by Man-PEG_{2000} lipoplexes. On the other hand, unlike Man-PEG_{2000} lipoplexes (Fig. 2B), the gene expression obtained by Man-PEG_{2000} bubble lipoplexes and US exposure was not suppressed in the presence of chlorpromazine (Fig. 4B), which is a clathrin-mediated endocytosis inhibitor [22]. These results agreed with the results of cellular association of pDNA (Supplementary Fig. 4B), and indicated that pDNA delivered by Man-PEG_{2000} bubble lipoplexes was directly introduced into the cytoplasm without mediating endocytosis by the gene transfection using Man-PEG_{2000} bubble lipoplexes and US exposure.

3.5. In-vivo gene transfection efficiency by Man-PEG_{2000} bubble lipoplexes and US exposure

As shown in Fig. 5A and B, the level of gene expression obtained by Man-PEG_{2000} bubble lipoplexes and US exposure was

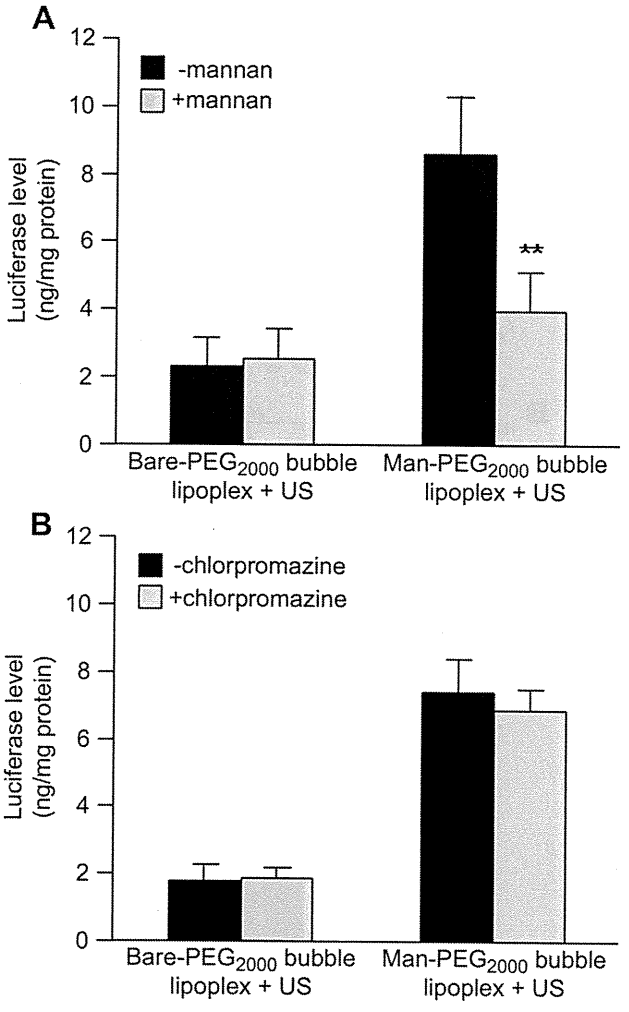

Fig. 4. Effects of mannan and chlorpromazine on gene expression by Man-PEG_{2000} bubble lipoplexes and US exposure in vitro. (A) The level of luciferase expression obtained by Bare-PEG_{2000} bubble lipoplexes with US exposure and Man-PEG_{2000} bubble lipoplexes with US exposure (5 μg pDNA) in the absence or presence of 1 mg/mL mannan at 24 h after transfection. $^{**}p < 0.01$, compared with the corresponding group of mannan. (B) The level of luciferase expression by Bare-PEG_{2000} bubble lipoplexes with US exposure and Man-PEG_{2000} bubble lipoplexes with US exposure (5 μg pDNA) in the absence or presence of 50 μM chlorpromazine at 24 h after transfection. Each value represents the mean + SD ($n = 4$).

500~800-fold higher than that by Man-PEG_{2000} lipoplexes, and also higher than that by Bare-PEG_{2000} bubble lipoplexes and US exposure or the conventional sonoporation method using naked pDNA and BLs in the liver and spleen, which are the targeted organs of mannose-modified carriers [27]. This enhanced gene expression in the liver and spleen was observed when bubble lipoplexes and US exposure were used for in-vivo gene transfer (Fig. 5C and D). Moreover, this gene expression obtained by Bare-PEG_{2000} bubble lipoplexes with US exposure or Man-PEG_{2000} bubble lipoplexes with US exposure in the liver and spleen remained higher than that by Bare-PEG_{2000} lipoplexes or Man-PEG_{2000} lipoplexes for at least 48 h, respectively (Fig. 5E and F). In addition, the gene expression was also enhanced in the US-exposed organ specifically following gene transfection by direct US exposure to the targeted organ after intravenous administration of Man-PEG_{2000} bubble lipoplexes (Supplementary Fig. 5). On the other hand, the increase of gene expression by bubble lipoplexes and US exposure was not observed in other organ such as lung, kidney and heart (Fig. 5G and H).

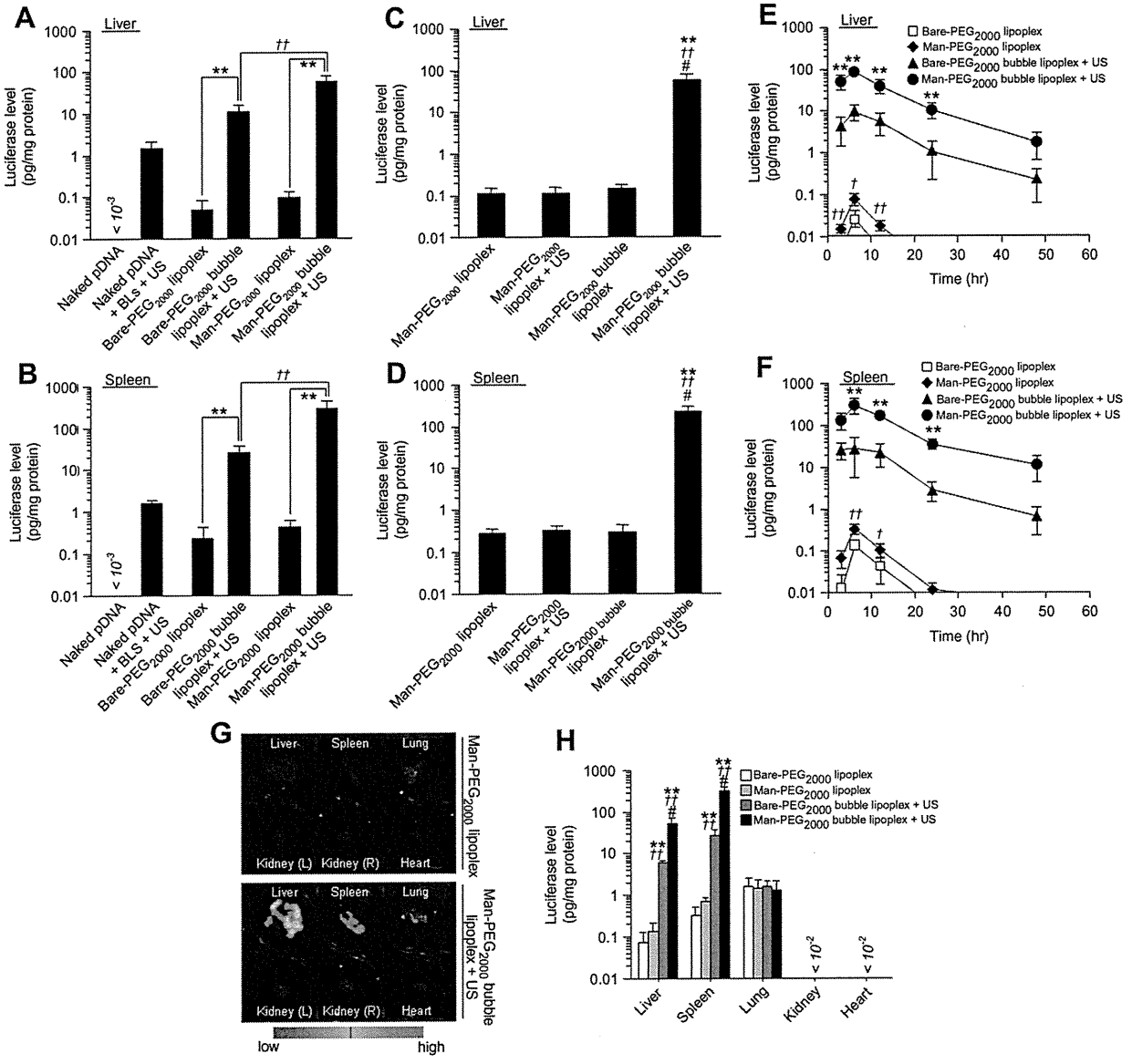

Fig. 5. Enhancement of mannose receptor-expressing cells-selective gene expression by Man-PEG_{2000} bubble lipoplexes and US exposure in vivo. (A, B) The level of luciferase expression obtained by naked pDNA, naked pDNA + BLs with US exposure, Bare-PEG_{2000} lipoplexes, Bare-PEG_{2000} bubble lipoplexes with US exposure, Man-PEG_{2000} lipoplexes and Man-PEG_{2000} bubble lipoplexes with US exposure (50 μg pDNA) in the liver (A) and spleen (B) at 6 h after transfection. Significant difference; **, $^{\dagger\dagger}p < 0.01$. (C, D) The level of luciferase expression obtained by Man-PEG_{2000} lipoplexes and Man-PEG_{2000} bubble lipoplexes with or without US exposure (50 μg pDNA) in the liver (C) and spleen (D) at 6 h after transfection. $^{**}p < 0.01$, compared with Man-PEG_{2000} lipoplex, $^{\dagger\dagger}p < 0.01$, compared with Man-$PEG_{2000}$ lipoplex + US, $^{\#\#}p < 0.01$, compared with Man-PEG_{2000} bubble lipoplex. (E, F) Time-course of luciferase expression in the liver (E) and spleen (F) after transfection by Bare-PEG_{2000} lipoplexes, Man-PEG_{2000} lipoplexes, Bare-PEG_{2000} bubble lipoplexes with US exposure and Man-PEG_{2000} bubble lipoplexes with US exposure (50 μg pDNA). Each value represents the mean ± SD ($n = 4$). $^{**}p < 0.01$, compared with Bare-PEG_{2000} bubble lipoplex + US, $^{\dagger}p < 0.05$; $^{\dagger\dagger}p < 0.01$, compared with Bare-$PEG_{2000}$ lipoplex. (G) In-vivo imaging photographs of luciferase expression in the isolated organs at 6 h after transfection by Man-PEG_{2000} lipoplexes and Man-PEG_{2000} bubble lipoplexes with US exposure (50 μg pDNA). (H) The level of luciferase expression in each organ at 6 h after transfection by Bare-PEG_{2000} lipoplexes, Man-PEG_{2000} lipoplexes, Bare-PEG_{2000} bubble lipoplexes with US exposure and Man-PEG_{2000} bubble lipoplexes with US exposure (50 μg pDNA). $^{**}p < 0.01$, compared with the corresponding group of Bare-PEG_{2000} lipoplex, $^{\dagger\dagger}p < 0.01$, compared with the corresponding group of Man-PEG_{2000} lipoplex, $^{\#\#}p < 0.01$, compared with the corresponding group of Bare-PEG_{2000} bubble lipoplex + US. Each value represents the mean + SD ($n = 4$).

3.6. *Targeted cell-selective gene transfection properties by Man-PEG_{2000} bubble lipoplexes and US exposure in vivo*

We investigated the mannose receptor-expressing cell selectivity of gene expression by transfection using Man-PEG_{2000} bubble lipoplexes and US exposure. In the liver, the level of gene expression in the hepatic NPCs expressing mannose receptors was significantly higher than that in the hepatic PCs following gene transfection by Man-PEG_{2000} bubble lipoplexes and US exposure (Fig. 6A). This difference in gene expression between the NPCs and PCs obtained by Man-PEG_{2000} bubble lipoplexes and US exposure was similar to that by Man-PEG_{2000} lipoplexes, although the level of gene expression in the NPCs and PCs was markedly higher. On the other hand, selective gene expression in the NPCs was not observed by Bare-PEG_{2000} bubble lipoplexes and US exposure.

In the spleen, the level of mRNA expression in the $CD11c^+$ cells, which are the splenic dendritic cells expressing mannose receptors, was significantly higher than that in the $CD11c^-$ cells following transfection by Man-PEG_{2000} bubble lipoplexes and US exposure (Fig. 6B). On the other hand, selective gene expression in the $CD11c^+$ cells was not observed by Bare-PEG_{2000} bubble lipoplexes and US exposure.

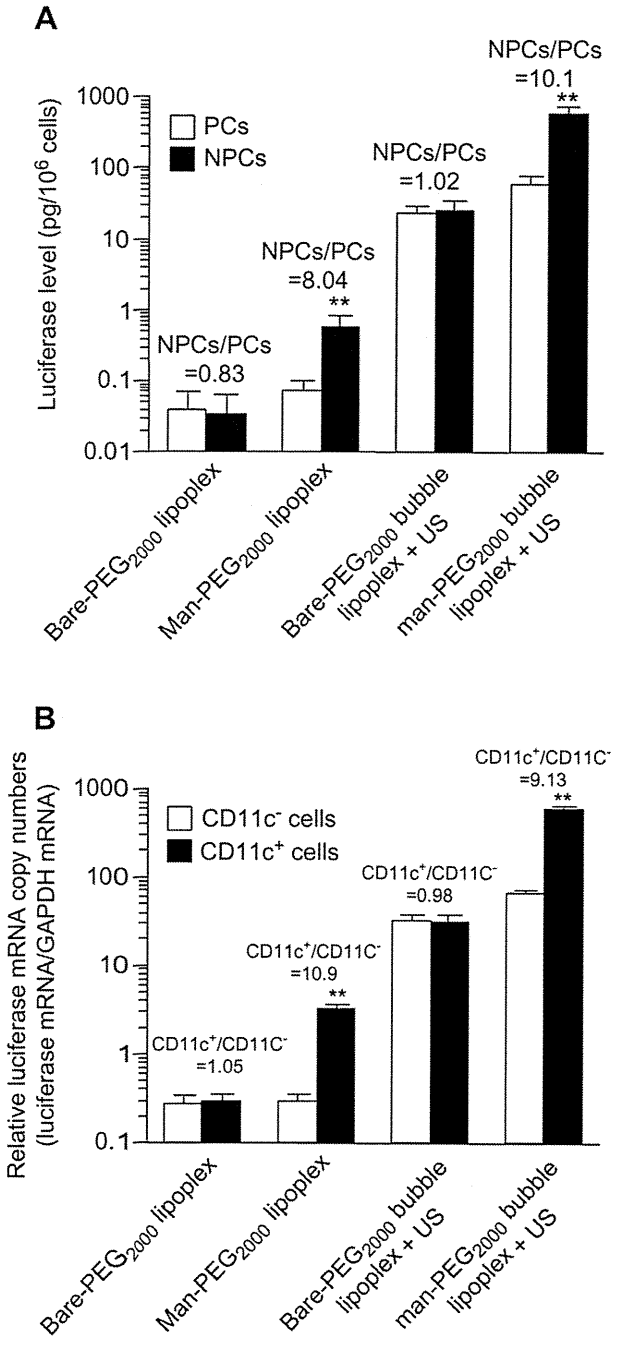

Fig. 6. Hepatic and splenic cellular localization of luciferase expression by Man-PEG_{2000} bubble lipoplexes and US exposure. (A) Hepatic cellular localization of luciferase expression at 6 h after transfection by Bare-PEG_{2000} lipoplexes, Man-PEG_{2000} lipoplexes, Bare-PEG_{2000} bubble lipoplexes with US exposure and Man-PEG_{2000} bubble lipoplexes with US exposure (50 μg pDNA). $^{**}p < 0.01$, compared with the corresponding group of PCs. (B) Splenic cellular localization of luciferase mRNA expression at 6 h after transfection by Bare-PEG_{2000} lipoplexes, Man-PEG_{2000} lipoplexes, Bare-PEG_{2000} bubble lipoplexes with US exposure and Man-PEG_{2000} bubble lipoplexes with US exposure (50 μg pDNA). $^{**}p < 0.01$, compared with the corresponding group of $CD11c^-$ cells. Each value represents the mean + SD ($n = 4$).

3.7. In-vivo distribution properties of pDNA by Man-PEG_{2000} bubble lipoplexes and US exposure

Next, to elucidate the mechanism of enhanced in-vivo gene expression using Man-PEG_{2000} bubble lipoplexes and US exposure, we investigated the effect on the tissue distribution of pDNA followed by gene transfection. In this study, Bare-PEG_{2000} bubble lipoplexes and Man-PEG_{2000} bubble lipoplexes constructed with radio-labeled pDNA were intravenously administrated, and then mice were subjected to external US exposure. As shown in Fig. 7, in the case of both bubble lipoplexes, the retention time of pDNA in the blood was slightly reduced and the distribution of pDNA delivered by bubble lipoplexes was significantly increased by US exposure in the liver and spleen (Fig. 7). Moreover, the amount of pDNA distributed in the liver and spleen by Man-PEG_{2000} bubble lipoplexes and US exposure (Fig. 7A) was higher than that by Bare-PEG_{2000} bubble lipoplexes and US exposure (Fig. 7B). On the other hand, no increase of pDNA distribution followed by US exposure was observed in the lung.

3.8. The liver toxicity by Man-PEG_{2000} bubble lipoplexes and US exposure

We examined ALT and AST activities in the serum to investigate the liver toxicity by gene transfection using Man-PEG_{2000} bubble lipoplexes and US exposure. ALT and AST activities in the serum were increased by gene transfection using Bare-PEG_{2000} lipoplexes and Man-PEG_{2000} lipoplexes. On the other hands, the increase of ALT and AST activities was not observed by gene transfection using Bare-PEG_{2000} bubble lipoplexes and Man-PEG_{2000} bubble lipoplexes with US exposure (Fig. 8).

3.9. Antigen presentation on MHC class I molecules in immunized splenic dendritic cells

To investigate the DNA vaccine effects by Man-PEG_{2000} bubble lipoplexes and US exposure, we prepared Man-PEG_{2000} bubble lipoplexes constructed with pDNA expressing OVA as a model antigen. Firstly, to investigate the antigen (OVA) presentation on MHC class I molecules in the splenic dendritic cells ($CD11c^+$ cells) by Man-PEG_{2000} bubble lipoplexes constructed with pCMV-OVA and US exposure, the splenic $CD11c^+$ cells isolated from once-immunized mice were co-incubated with CD8-OVA1.3 cells, which are T cell hybridomas with specificity for OVA. Following measurement of IL-2 to evaluate the activation of T cells, the IL-2 secretion from activated CD8-OVA1.3 cells co-incubated with the $CD11c^+$ cells isolated from mice immunized by Man-PEG_{2000} bubble lipoplexes and US exposure was the highest of all (Fig. 9A). This result indicates that DNA vaccination by Man-PEG_{2000} bubble lipoplexes constructed with pCMV-OVA and US exposure can induce significantly high $CD8^+$-T lymphocyte activation.

3.10. Antigen-specific cytokine secretion from immunized splenic cells

We evaluated the OVA-specific cytokine secretion from the splenic cells immunized by Man-PEG_{2000} bubble lipoplexes constructed with pCMV-OVA and US exposure. Following optimization of immunization schedule, it was shown that a 2 week interval was necessary to achieve the same level of gene expression as former transfection in the spleen (Supplementary Fig. 6) and at least three times immunization was necessary to effective anti-tumor effects by DNA vaccination using this method (Supplementary Fig. 7). Therefore, the immunization to mice was performed according to the protocol shown in Fig. 9B. As shown in Fig. 9C, in the presence of OVA, the highest amount of IFN-γ (Th1 cytokine) was secreted from splenic cells harvested from mice immunized with Man-PEG_{2000} bubble lipoplexes and US exposure. On the other hand, no secretion of IFN-γ was observed in any of the groups in the absence of OVA. Moreover, the secretion of IL-4 (Th2 cytokine) was not increased in any of the groups both in the presence or absence of OVA (Fig. 9C). These results suggest that immunization by Man-PEG_{2000} bubble lipoplexes constructed with